Quaternary Science Reviews 29 (2010) 2238–2260

Contents lists available at ScienceDirect

Quaternary Science Reviews

journal homepage: www.elsevier.com/locate/quascirev

Widespread aggradation in the mountainous catchment of the Alaknanda–Ganga River System: timescales and implications to Hinterland–foreland relationships

Yogesh Ray, Pradeep Srivastava*

Wadia Institute of Himalayan Geology, 33 GMS Road, Dehradun 248001, India

ARTICLE INFO

Article history:
Received 23 October 2009
Received in revised form
10 April 2010
Accepted 24 May 2010

ABSTRACT

Cut-and-fill type fluvial terraces are ubiquitous in the Lesser Himalayan zone of the Alaknanda–Ganga (Ganges) rivers system, which flows perpendicular to Himalayan lithotectonic units and traverses a steep climatic gradient. Lithofacies analysis of the sedimentary sequences of cut-and-fill terraces indicated that the valley aggradation took place via (1) channel bar development and excess sediment supply, (2) debris flows composed of mixed rounded to sub-rounded lithoclasts, resulting from episodic high intensity rainfalls in the upper catchment or (3) debris flows or rockfalls generated by local landslides. The luminescence chronology indicates that valley aggradation took place in two phases: ~49–25 ka and 18–11 ka. The incision of the fill started soon after 11 ka. Paleoclimatic records from marine sediments indicate that the aggradation and incision in the Alaknanda–Ganga River has oscillated in-phase with global climatic variations. Glaciation–deglaciation processes in the upper catchment produced huge amounts of sediment between 63 and 11 ka, which was fluvially transferred to the lower valley via several cycles of erosion and deposition, leading to extensive aggradation. The climatic amelioration at ~11 ka and the completion of deglaciation processes led to increased fluvial discharge and decreased sediment supply, conditions conducive for incision of the alluvial fills. Records from the Indo-Gangetic plain and the Ganga Delta demonstrate that the phase of aggradation was regional but that incision in the foreland started at least 2–3 ka later, after 7 ka.

Bedrock incision rates, as calculated from dated alluvial covers of terraces that are separated by bedrock steps, are spatially variable and fall within the range of rates reported from across the Himalaya. These estimated rates, however, are higher than the basin average erosion rates calculated using isotopic mass balance in riverbed sediments. This study suggests that during the last 50 ka river dynamics in the Himalayas were dominated by monsoon variability and the role of tectonic activity was limited to bedrock incision in few reaches only.

1. Introduction

Fluvial terraces are often used to decipher controlling factors and timescales of river aggradation and incision like regional atectonic uplift (Maddy, 1997; Bridgland, 2000) and tectonic uplift and climate (Srivastava and Misra, 2008; Srivastava et al., 2008). Existing research suggests that valley-scale aggradation may represent climatic impact whereas fluvial incision into the bedrock equals the long-term uplift rate and thus the local rise of the incision rate can be interpreted as an effect of vertical motion along the active tectonic discontinuities and/or increased hydraulic efficiency (Pazzaglia et al., 1998; Hancock and Anderson, 2002; Bridgland and Westaway, 2007). The aggradation history of rivers has also been studied to understand the response of glaciation and deglaciation in evolution of paraglacial landscape and the lower reaches of glaciated rivers (Church and Slaymaker, 1989; Schildgen et al., 2002). The Himalaya, an active thrust fold orogenic belt, formed due to the continent–continent collision between the Asian and the Indian plates, is drained by several north and south flowing rivers: the Ganga (Ganges), the Yamuna and the Brahmaputra. The Ganga river system, governed by a single climatic forcing factor, i.e. the Indian Summer Monsoon (ISM), originates in the higher Himalaya and cuts through the tectonic discontinuities of this orogen and traverses the E–W trending foreland before it finally flows into the Bay of Bengal. Therefore, if studied in detail, this river has the potential to provide a synoptic view of fluvial responses to changing climate, to a rising orogen and upland control on the development of the foreland. Fluvial terraces are ubiquitous in the Himalayan catchment and have been extensively studied to understand (1) the orogenic process at the mountain front (Laveì

* Corresponding author.
E-mail address: Pradeep@wihg.res.in (P. Srivastava).

0277-3791/$ – see front matter © 2010 Elsevier Ltd. All rights reserved.
doi:10.1016/j.quascirev.2010.05.023

and Avouac, 2000; Mukul et al., 2007; Srivastava and Misra, 2008), (2) climate–tectonic relationships in the evolution of the Himalaya (Hodges et al., 2004; Pratt et al., 2004; Thiede et al., 2004), and (3) fluvial responses to climatic changes (Bookhagen et al., 2005; Srivastava et al., 2008, 2009). In the Himalayan foreland the Ganga river has formed three distinct levels of regional surfaces that have been studied for their stratigraphic evolution, climate and tectonic interpretations (Singh, 1996; Singh et al., 1997; Srivastava et al., 2003a,b,c; Sharma et al., 2004a,b; Gibling et al., 2005; Tandon et al., 2006; Sinha et al., 2007). Based on limited chronological data, a conceptual relationship that explains the mechanism, processes and timescales of sediment transfer from the Himalaya to foreland to delta has been visualized by Goodbred (2003). Lacking in these studies is a synoptic view that reconciles the existing records from the mountain range and its foreland and the new dataset that explains aspects of the thrust and fold belts globally. The Late Quaternary has seen significant shifts in climate and it seems likely that the hydrology, sediment production, and carrying capacity of tropical–subtropical river systems such as the Ganga would have also varied at a similar frequency to climate (Goodbred, 2003). In this paper we show, by making use of evidence from river terraces, sedimentology of valley fills and luminescence dating, that in the Ganga river system sediment production, aggradation and subsequent incision have oscillated with climate change. We present new chronological, geomorphological and sedimentological data from terraces in the Himalayan catchment. Furthermore, we attempt correlation of the aggradation and incision events with global climatic changes.

2. The Ganga River: regional setting

2.1. Geological background

The Alaknanda–Ganga River flows through two distinct continental-scale geomorphic features: (1) the Himalaya, a tectonically active orogen and (2) the Ganga Foreland, formed by the downward flexure of the underthrusting Indian Plate. The northern part of the Alaknanda–Ganga catchment drains through the Himalayan thrust belt and the southern part flows across the vast Ganga alluvial plain of the Himalayan foreland (Singh, 1996; Singh et al., 2007). In the Himalaya, the Alaknanda and Bhagirathi are the two main tributaries, which are in general characterized by glaciers feeding their headwaters, by gorges, and well formed terraces. In the pre-confluence region from the headwaters upstream of Deoprayag, the paper focuses on the Alaknanda River, and thereafter, the Ganga trunk channel is followed from the confluence to Varanasi in the central Ganga foreland (Fig. 1).

In the Himalaya, the Alaknanda River flows perpendicular to the Himalayan thrusts. These thrusts decrease in age southwards; the oldest and northernmost tectonic zone is the Indus Tsangpo Suture Zone (ITSZ), followed by the South Tibetan Detachment (STD), the Main Central Thrust (MCT) and the Main Boundary Thrust (MBT). The river leaves the orogen after crossing the Himalayan Frontal Thrust (HFT). Fig. 2 shows the thrust boundaries and lithotectonic units traversed by the Alaknanda–Ganga Rivers. The Alaknanda–Ganga River catchment cuts through the rocks of the Tethys Himalayan Sequence (THS), the Higher Himalayan Crystalline (HHC) and the Lesser Himalayan sedimentaries (LHS). The rocks exposed in the Alaknanda Valley north of the STDS are called the Tethys Himalayan Sequence (THS), composed of fossiliferous sedimentary to metasedimentary lithologies. Rocks of the Higher Himalayan Crystalline (HHC) occur between the STD and MCT, consisting of medium to high grade metamorphic rocks. Lesser Himalayan (LHS) rocks are exposed between the MCT and MBT and comprise carbonaceous shale, limestone, dolomite, quartz arenite and metavolcanic rocks, as well as argillite. The North Almora Thrust (NAT) is an out-of-sequence thrust that emplaces HHC rocks over the LHS sequence. South of the MBT lies the Sub Himalaya consisting of Lower Tertiary and Siwalik rocks, consisting of sandstone, conglomerate, mudstone and subordinate amount of

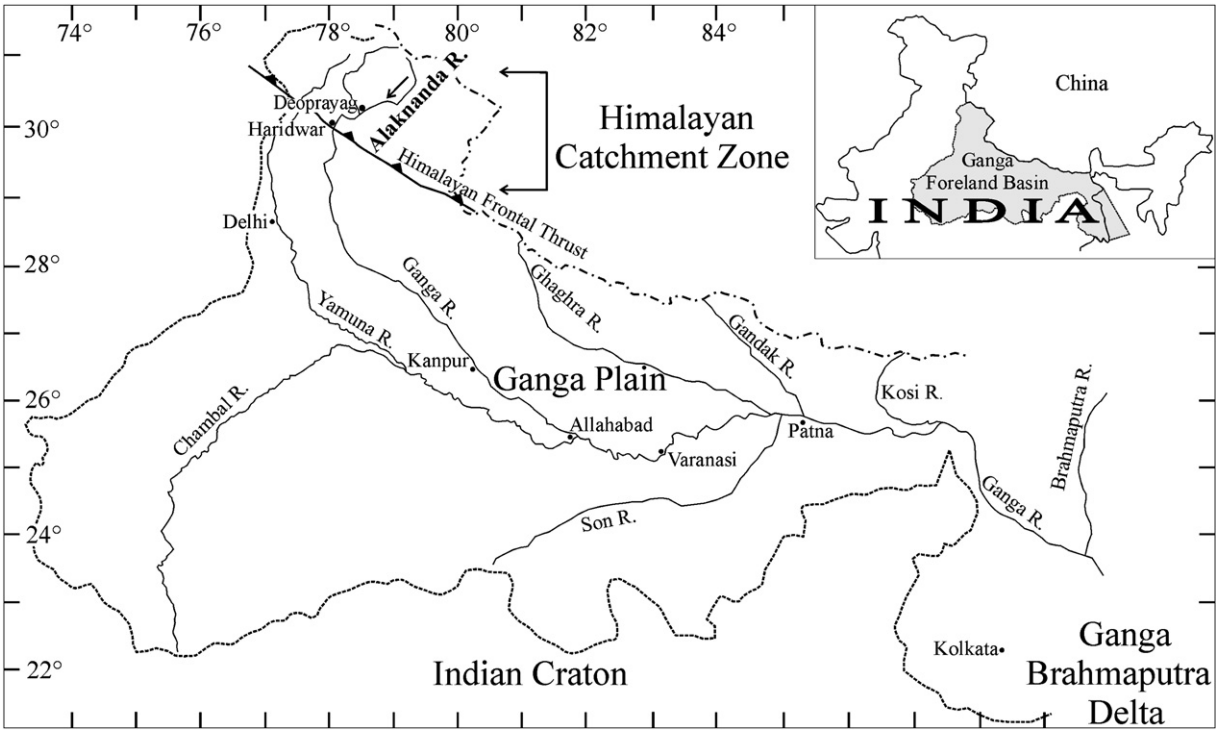

Fig. 1. The Alaknanda–Ganga river system flowing through the Himalaya and the Ganga foreland to the Ganga–Brahmaputra Delta. The Alaknanda tributary flows N–S to a confluence near Josimath (see Fig. 2).

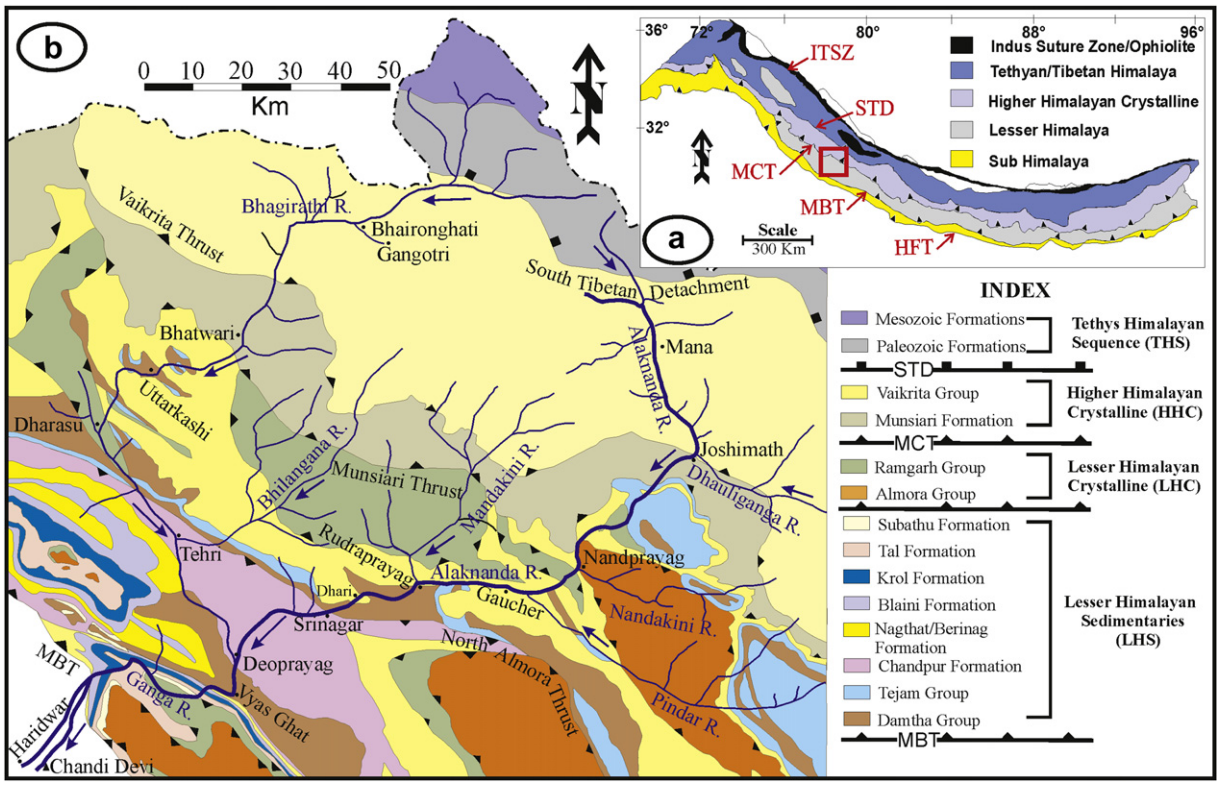

Fig. 2. (a) Geological map of the Akaknanda–Ganga river catchment in the Himalaya. (b) Geological cross-section as exposed along the river (modified after Srivastava and Ahmad, 1979).

limestone restricted mainly to the Lower Tertiary packages. Sub Himalayan rocks are thrusted over the sediments of the modern Ganga foreland basin along the HFT. Details on the formations and lithology are discussed in Valdiya (1980) and Srivastava and Ahmad (1979). Various thrusts exposed in the Alaknanda Valley define a strong geomorphological break marked by knick points in the river profile, incised valleys in the upstream sectors, and significant terrace development and more open valleys to the south (Pal, 1986). At places along the river, several transverse faults, such as the Alaknanda fault, the Kaliyasaur fault and the Deoprayag fault, play an important role in the formation of the wide valleys and river terraces. The Alaknanda fault extends in an E–W direction on the right bank of the Alaknanda between Tilwara, Langasu and Rudraprayag. The Chamoli earthquake (on 29 March, 1999) was generated along this fault and the fault plain solution and geological investigations indicated that the Alaknanda fault is a thrust fault with a shallow dip of 15–20° (Kumar and Agarwal, 1975; Rawat, 1979; Rawat and Varadarajan, 1979; Thakur, 2004). The Kaliasaur fault, trending WNW–ESE in the west and NE–SW in the east, is another major fault in the area that is marked by alignment of streams across the water divide and by extensive landslides. The dip of the fault ranges from 50° to 90° (Jha, 1992). Movements along this fault have produced a prominent quartzitic fault gouge.

The Ganga River debouches into its foreland after crossing the HFT at Haridwar. The foreland basin that is formed above the underthrusting Indian plate shows all the major components of an active foreland, including an adjacent orogen (the Himalaya), a deformed and uplifted foreland basin adjacent to the orogen (the Siwalik Hills), a depositional basin (the Ganga Plain) and a cratonic peripheral bulge (the Bundelkhand–Vindhyan plateau) (Fig. 3). Sastri et al. (1971) and Rao (1973) provide an account of the basement structure of the Ganga Plain and suggest that the basin is traversed by N–S trending basement highs and lows that are transverse to the orogen.

2.2. River valley profile and geomorphology

The Alaknanda River originates from the Satopanth glacier at a height of 3641 m a.s.l. (above sea level) and meets the River Bhagirathi at Deoprayag (459 m a.s.l.); it has a total catchment area of 10,237 km^2. On the basis of geomorphology and climate it can be divided into three major reaches from north to south: (1) the Upper Reach, arid–semi-arid, glaciated with 'U'-shaped valleys lined with moraine ridges, largely falls north of the MCT in the altitude range of >6500–2600 m a.s.l. The mapping of moraines in this reach indicates that the elevation of glacier snouts varied from 2604 m a.s.l. (~63 ka BP) to 3550 m a.s.l. (21–15 ka BP) to 3850 m a.s.l. at present (Sharma and Owen, 1996; Nainwal et al., 2007). (2) The Middle Reach is characterized by steep slopes, with 'V'-shaped river valleys forming deep gorges. It is located from the MCT zone to ~60 km south in the Lesser Himalaya. This zone, between 2600 and 1200 m a.s.l., forms an orographic barrier to the northward advancing Indian Summer Monsoon and is characterized by high rainfall and erosion (Wasson et al., 2008). (3) Wider 'V'-shaped valleys with lower channel and slope gradients characterize the Lower Reach. This part of the river ranges from ~1200 m a.s.l. in the Lesser Himalaya to ~250 m a.s.l. near the HFT at the mountain front. Impressive cut-and-fill staircases and terraces with underlying bedrock steps distinguish this reach, which we studied in detail at 15 locations between Nandprayag and Chandi Devi. Fig. 4A shows the longitudinal profile of the Alaknanda–Ganga River system and Fig. 4B the tectonic discontinuities and locations of the study sites. The steepness index, calculated along the longitudinal river profiles of the Alaknanda River, indicates higher values in the Nandprayag and Karnprayag sector (201 and 205 respectively), falling to 131 at Srinagar (Tyagi et al., 2009). The valley gradient in the mountains ranges between 10 and 3 m/km and declines to 1.7 m/km at the mountain front, where the river enters the foreland, and in the middle part of the Ganga foreland the gradient

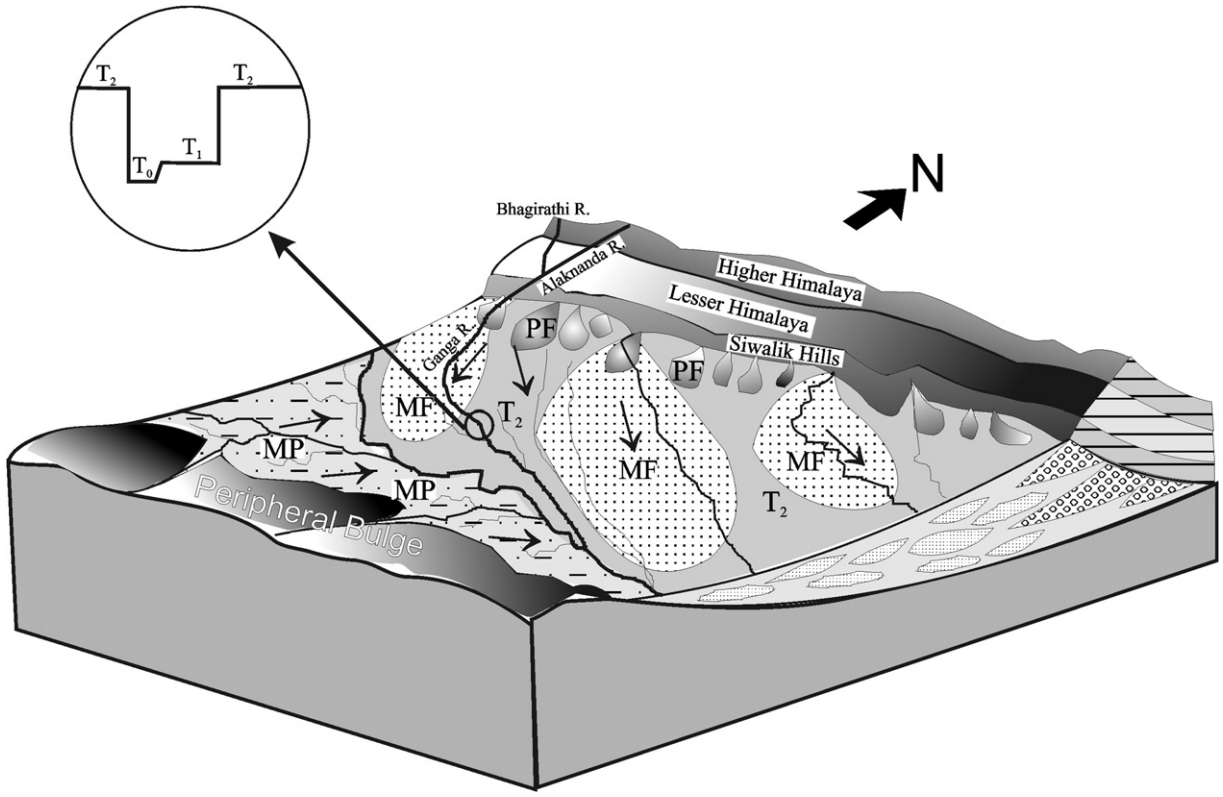

Fig. 3. Schematic diagram showing geomorphic features of the Ganga Plain (after Singh, 1996; not to scale). T2-Upland Terrace Surface, MP-Marginal Plain Upland Surface, MF-Megafan Surface, T1-River Valley Terrace Surface, PF-Piedmont Fan Surface, T0-Active Flood Plain Surface.

further decreases to 16 cm/km (Singh et al., 2007). This decrease in channel gradient is in general accompanied by widening of the active channel and a significant decrease in stream power. The width, slope and discharge data, available for limited locations, suggests that the stream power of the river within the mountains varies from >900 to 200 W/m^2 in the mountains, reducing in the foreland to between 60 and 10 W/m^2. The data used in stream power calculations is given in Table 1. The Ganga River in the foreland is incised into the upland surface and is flanked by vertical cliffs. Synoptic studies of the Ganga Plain have identified regionally significant geomorphic surfaces (Singh, 1996; Fig. 3), namely (1) the Upland Interfluve Surface (T-2), (2) the Marginal Plain Upland Surface (MP), (3) the Megafan Surface (MF), (4) the River Valley Terrace Surface (T-1), (5) the Piedmont Fan Surface (PF) and (6) the Active Flood Plain Surface (T-0).

3. Methods

Detailed mapping of the terraces in the mountain catchment was carried out with the help of a total-station survey, and Survey of India (SOI) topographic maps at the scales of 1:25,000 and 1:50,000. A Digital Elevation Model (DEM) of the Alaknanda catchment was constructed using Shuttle Radar Topographic Mission (SRTM, 2000) data of interest processed using the Topographic module of ENVI and Global Mapper. SRTM data with a resolution of 3 arc seconds (90 m pixel resolution) was also used as basic data to map the Alaknanda catchment. The datum of the SRTM data was changed from 'Geographic Latitude Longitude' to 'Everest' and projection 'WGS 84' to 'Lambert conformal conic' so that the measurement unit changed from degrees to meters. In addition the surface area was calculated using the 3D analyst tool of ARC GIS 9.3 (Software of Environmental System Research Institute (ESRI)). The surface area vacated during the deglaciation of different stages was also calculated (discussed later). Extensive field studies were carried out to check the geological map, to map the terraces and document their sedimentary architecture. The elevations of different terrace surfaces were measured with the help of total-station survey where the reference heights above mean sea level were ascertained using spot heights given in SOI toposheets and THALES hand held Global Positioning System (GPS with accuracy $\pm$3 m). The accuracy of the GPS was checked using several spot heights and benchmarks provided by SOI toposheets. Several levels of fluvial terraces were identified using field surveys. The valley cross-sections were drawn using the SRTM and field data.

Studies of the style of valley aggradation were based on lithofacies identification and preparation of vertical and lateral sedimentary logs in the field. Several exposed sections along the river and excavated trenches were used for detailed sedimentological studies. The lithofacies classification is based on observations of gravel lithology, roundness, size, matrix proportion, bioturbation, and degree of iron staining and grain size. Lithoclast composition and texture was visually ascertained using the 1 $\times$ 1 m grid overlays.

Optically Stimulated Luminescence (OSL) dating of the top and the lowermost units of terrace sediments was carried out to deduce the timing and duration of river aggradation and the rate of incision of alluvium and bedrock. The age at the lowest stratigraphic unit marks the initiation of terrace aggradation and that at or near the top provides the time when the terrace surface was abandoned and the river incised to subsequent lower surface. Samples were collected using opaque stainless steel pipes. This technique relies on the premise that, prior to burial, geological luminescence stored in the minerals was zeroed by daylight exposure during erosion and transportation (Aitken, 1998). A basic concern in OSL dating of sediments is the extent to which the geological luminescence at the time of burial was reduced and any error in this would imply an over-estimation of age (Duller, 2008). Fluvial sediments in the

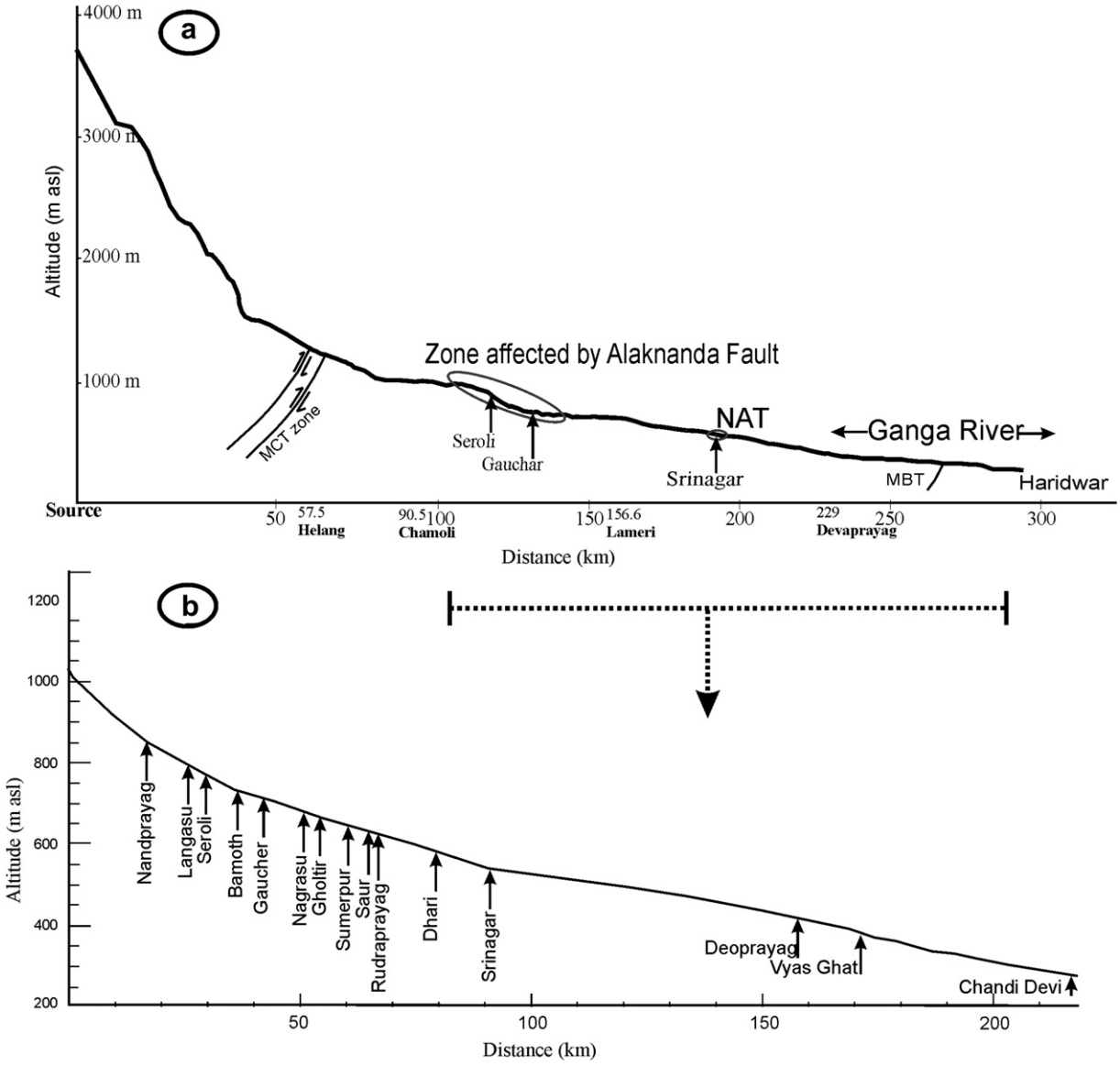

Fig. 4. (a) Geomorphic profile of the Alaknanda–Ganga River from source to mountain exit. Note the zone affected by Alaknanda fault. (b) Profile of the reach and locations studied in detail.

Himalaya are generally deposited under high-energy turbulent conditions and thus carry a possibility of poor and inhomogeneous zeroing. The uncertainty arising due to this is tackled by reducing the size of aliquots and by considering the lowest palaeodoses in age estimation (Srivastava et al., 2006, 2008, 2009). Poor or inhomogeneous luminescence bleaching of sediments is expressed as a wide scatter in palaeodose estimates and the lower palaeodoses that are considered here represent the most bleached part of the sediment (Preusser et al., 2009). Similarly, usage of small subsamples (aliquots) increases the possibility of detecting poorly bleached grains (Wallinga, 2002; Srivastava et al., 2006). However, the published OSL chronology for the rivers of the Himalaya highlights the problem of low luminescence sensitivity of quartz grains, which limits the possibility of reducing the aliquot size, and also the poor photon counts puts constraints on the number of aliquots that can be used meaningfully in age estimation (Jaiswal et al., 2008).

Table 1
Stream power of the river calculated at different locations. Note that from the mountains to the foreland the values decrease significantly (Data from Singh et al., 2007 and from various sources).

River/Tributary/Segment	Location	Mean monsoon discharge (m^3/s)	Channel width (m)	Channel gradient	Unit stream power (W/m^2)
Alaknanda/mountain	Srinagar	1900	154	0.0015	181
Alaknanda/mountain	Deoprayag	1775	75	0.002	463
Ganga/mountain exit	Haridwar	5860	500	0.0017	196
Ganga/Ganga plains	Garhmukteshwar	5800	400	0.0003	43
Ganga/Ganga plains	Kanpur	6317	1000	0.00016	10
Ganga/Ganga plains	Allahabad	24,131	750	0.00016	50
Ganga/Ganga plains	Varanasi	21,262	4000	0.00012	63

Feldspar contamination in quartz is another problem, as this mineral, being brighter in terms of luminescence emission, masks the quartz signal. Infrared-Stimulated Luminescence (IRSL) performed on the sample tends to reduce the feldspar signal to acceptable limits, approaching the quartz signal only marginally (Jain and Singhvi, 2001). In the case of clean quartz samples (no feldspar contamination), the IRSL output will be limited to 100–150 photon counts. Additionally a fault gouge at Kaliyasaur was dated to ascertain tectonic activity along this fault. The dating of the fault gouge is based on the assumption that during faulting the temperature along the fault plane rose sufficiently to reset the OSL signal; hence the date represents the last major movement along the fault (Banerjee et al., 1999). However, in the present case, no mechano-luminescence study to assure the zeroing of the geological luminescence in the fault gouge has been done, so the age should be considered as evidence of tectonic activity rather than an absolute age of the activity.

The quartz fraction from samples was extracted by sequential chemical treatment, following Srivastava et al. (2006). The fraction was sieved to separate the 90–150 μm size range and etched using 40% HF for 80 min, followed by 12 N HCl treatment for 40 min to remove alpha-irradiated surface layers. IRSL measurement was performed on every sample to check the feldspar contamination. The samples showing IRSL counts more than 100 were subjected to the additional step of density separation and HF etching for 20 min. The grains were mounted on stainless steel disks using Silko-Spray silicone oil. Luminescence measurements were made on a Riso TL/OSL-12 system with an array of blue LEDs as a source for stimulation. Schott BG-39 and Hoya U-340 optical filters in front of an EMI 9235 QA photomultiplier tube were used for photon detection.

OSL was recorded for 40 s at 125 °C. A $^{90}Sr/^{90}Y$ beta source delivering a dose rate of 5.5 Gy/min was used for irradiation. A 5-point single aliquot regeneration (SAR) protocol, suggested by Murray and Wintle (2000), was used to determine the paleodose. An additional step of IRSL cleaning (for 100 s at 60 °C) was introduced before every OSL measurement. This was done to reduce any signal coming from feldspar (Jain and Singhvi, 2001). A preheat of 220 °C/10 s and a cut heat of 160 °C for test doses were used. 30–40 discs were used for measurement out of which the weighted mean of the lowest 20% paleodose values were used for age calculations (Galbraith et al., 1999; Srivastava et al., 2009). The OSL measurements were done for 40 s at 125 °C. The paleodose estimate is based on aliquots with a recycling ratio of 1.1–0.9. The initial 2 channels (1 channel = 0.16 s of OSL measurement) of the shine-down curve were used for analysis. Uranium, thorium and potassium concentrations were determined by XRF analysis.

4. Results

4.1. Luminescence chronology

The chronological framework of the study is based on 38 luminescence dates, 28 new ages and the rest after Srivastava et al. (2003a,b, 2008) and Tandon et al. (2006). Single Aliquot Regeneration (SAR) analysis based on terrace samples yielded a positively skewed dose distribution, which suggests partial bleaching (Fig. 5).

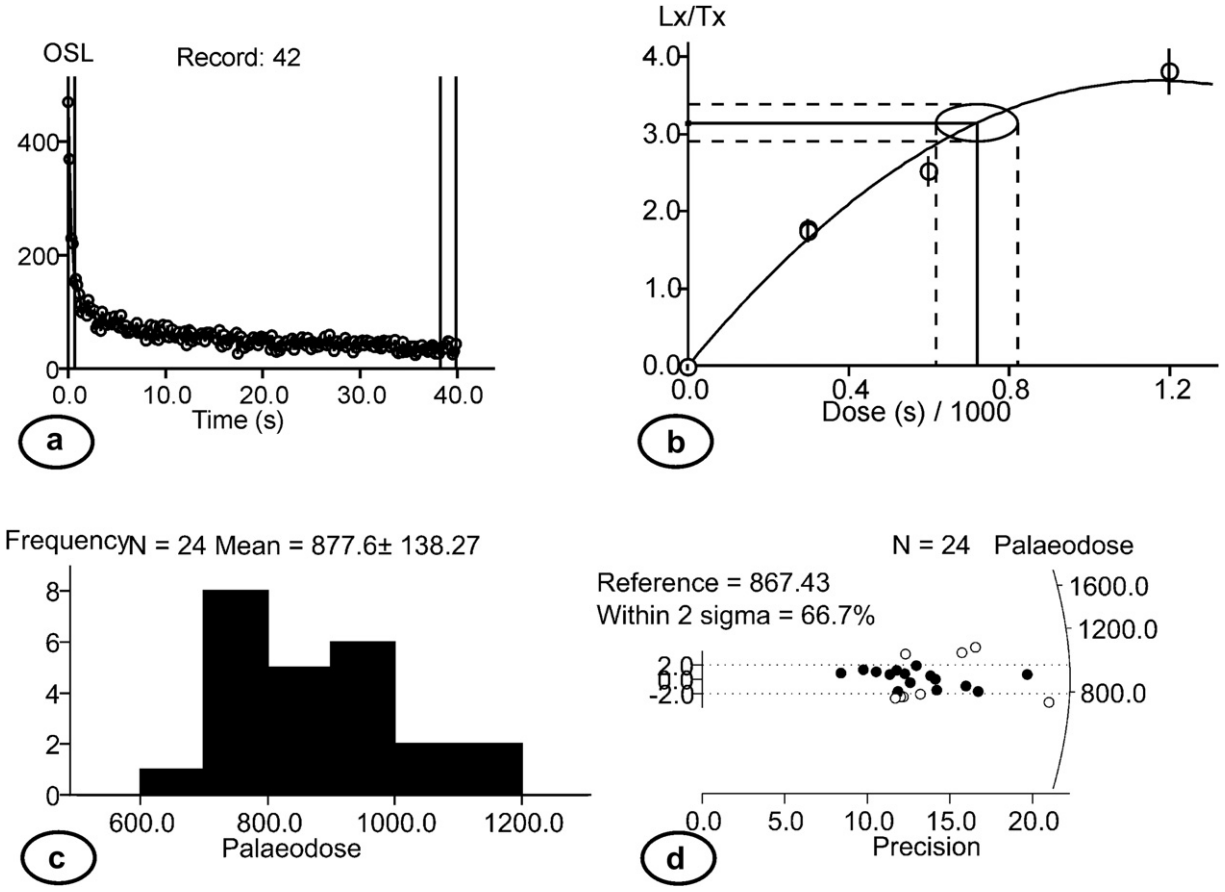

Fig. 5. (a) The OSL shine-down curve of a natural signal from the sample LD-487. (b) The dose–growth curve of the same sample constructed from single aliquot of 7 mm diameter having ~800 grains on average. Due to low sensitivity, analysis of smaller aliquots less than that was not carried out. (c) Dose distribution of the equivalent doses (De's) from the very samples. The distribution indicates inhomogeneous bleaching of the sediment. (d) Radial plot showing the dose distribution.

This implied the need to use lower paleodoses for age analysis (Olley et al., 1998; Srivastava et al., 2009). In the present study, an average from the lowest 20% of paleodoses (4–6 discs) were used for age calculation in young samples. The age and dosimetery data of all the samples is given in Table 2. The sections at Nandprayag yielded an age of 27 ± 3 ka (LD-446) and at Langasu 16 ± 2 ka (LD-447). The alluvial fill of the Seroli section yielded an age of 49 ± 1 ka (LD-487). Sample LD-258, collected from Bamoth, yielded an age of 16 ± 2 ka. At Gaucher, samples near the base of the section yielded an age of 37 ± 4 ka (LD-254), from 30 m higher the age was 17 ± 2 ka (LD-255) and from near the top it was13 ± 1 ka (LD-257). Samples collected from the base of terraces T-1 and T-2 at Nagrasu were dated to 13 ± 2 ka (LD-324) and 34 ± 6 ka (LD-449). The sedimentary fill at Gholtir yielded ages of 40 ± 4 ka (LD-325) and 11 ± 2 ka (LD-326). Further downstream, an 11 m alluvial fill at Sumerpur gave an age of 17 ± 3 ka (LD-332) from near its base. The top of a profile at Saur village gave an age of 11 ± 3 ka (LD-451) and ~3 km further downstream, at Rudraprayag, three samples from the base to the top of first profile yielded ages of 41 ± 5 ka (LD-335), 35 ± 7 ka (LD-334) and 18 ± 3 ka (LD-333). From ~20 km further downstream of Rudraprayag (N30°15′04.4″ E78° 55′31.0″) a fault gouge was dated to 85 ± 10 ka (LD-490). At Dhari, a 55 m thick sediment fill yielded an age of 27 ± 2 ka (LD-376) at 13 m and 20 ± 2 ka (LD-377) at 11 m below the top. At Srinagar, alluvial fills located on two levels of bedrock steps were dated. The fill overlying the upper level step yielded an age of 25 ± 2 ka (LD-329) and that overlying the lower is dated to between 17 and 14 ka (LD-207 and LD-327). A similar age of 11 ± 2 ka (LD-381) was obtained from the top of the upstream continuation of this fill at Supana. At Deoprayag, a 79 m thick fill terrace yielded an age of 21 ± 2 ka (LD-19) near its base and 18 ± 2 ka (LD-20) at 37 m from the top, 12 ± 2 ka (LD-19A) at 33 m from the top and, from near the top, 10 ± 2 ka (LD-20A). Similarly, a section at Vyas Ghat yielded an age of 18 ± 2 ka (LD-567). Finally, in the frontal belt of the Himalaya, in the Siwalik

Table 2
Radioactive element concentrations, dose rate, Paleodose and ages of the samples collected from paleoflood and terrace deposits. Average of least 10% paleodoses were taken Moisture content of 10 ± 5% was assumed for all samples and cosmic ray Gamma contribution was calculated after Prescott and Stephan (1982).

S. no	Lab. no	Depth (m)	Location		Cosmic dose rate (μGy/a)	U (ppm)	Th (ppm)	K (%)	Paleodose (grey)		Dose rate (Gy/ka)	Age (ka)	
			Longitude	Latitude					Mean	Least		Mean	Least 20%
Nandprayag													
1	LD-446	6	E79°18′55″	N30°19′59.7″	161.6	3.4	14.3	1.4	96 ± 24	81 ± 7	3.0 ± 0.2	31 ± 8	27 ± 3
Langasu													
2	LD-447	4.5	E79°18′01.5″	N30°17′42.1″	173.2	1.2	13	1.8	140 ± 66	45 ± 4	2.8 ± 0.2	49 ± 23	16 ± 2
Seroli													
3	LD-487	10	E79°14′16.8″	N30°16′47.2″	141.6	1.3	6.9	0.6	85 ± 16	69 ± 4	1.4 ± 0.09	61 ± 12	49 ± 4
Bamoth													
4	LD-258	5	E79°10′17.1″	N30°16′10.7″	164.5	2.9	12.5	1.6	59 ± 11	46 ± 3	3.0 ± 0.2	20 ± 4	15 ± 2
Gaucher													
5	LD-254	24	E79°09′34.1″	N30°17′53.4″	121.1	2.9	7.4	1.5	96 ± 10	94 ± 9	2.5 ± 0.1	38 ± 5	37 ± 4
6	LD-255	1.5	E79°09′34.1″	N30°17′53.4″	199.6	5.3	17.5	2.2	107 ± 42	74 ± 10	4.4 ± 0.2	24 ± 10	17 ± 2
7	LD-256	3	E79°09′54.2″	N30°17′13.4″	181.4	6.4	21.7	1.7	148 ± 16	130 ± 4	4.4 ± 0.3	33 ± 4	29 ± 3
8	LD-257	1.5	E79°09′50.0″	N30°16′55.7″	202.7	4.4	17	1.8	54 ± 4	48 ± 3	3.8 ± 0.2	14 ± 2	13 ± 1
9	LD-452	1	E79°09′26.3″	N30°17′26.2″	214	1	9.5	1.2	38 ± 9	33 ± 2	2.1 ± 0.1	18 ± 4	16 ± 2
Nagrasu													
10	LD-324	18	E79°07′04.7″	N30°18′09.2″	126.6	3.3	14.7	1.4	65 ± 16	41 ± 4	3.0 ± 0.2	21 ± 5	13 ± 2
11	LD-449	6	E79°10′04.1″	N30°17′47.1″	161.2	2.6	16.3	1.6	170 ± 55	104 ± 16	3.0 ± 0.2	53 ± 18	34 ± 6
Gholtir													
12	LD-325	6.5	E79°05′34.8″	N30°18′04.4″	155.2	2.1	6.6	1.3	106 ± 11	89 ± 2	2.2 ± 0.1	48 ± 6	40 ± 4
13	LD-326	5	E79°05′34.8″	N30°18′08.9″	164.2	3.7	6.1	1.2	60 ± 22	28 ± 4	2.4 ± 0.2	24 ± 9	11 ± 2
Sumerpur													
14	LD-332	7	E79°01′44″	N30°18′09.3″	151.8	4.9	8.8	1.5	59 ± 12	50 ± 9	3.1 ± 0.2	19 ± 4	17 ± 3
Saur													
15	LD-451	6	E79°00′42″	N30°17′52.0″	162.1	2.1	13.6	1.4	69 ± 30	29 ± 8	2.7 ± 0.1	25 ± 11	11 ± 2
Rudraprayag													
16	LD-335	11	E78°59′42.4″	N30°18′02.2″	137.7	2	15.2	1.1	122 ± 17	102 ± 11	2.5 ± 0.2	49 ± 8	41 ± 5
17	LD-334	4	E78°59′42.4″	N30°18′02.2″	171.8	4.2	12.9	1.4	137 ± 32	111 ± 18	3.1 ± 0.2	43 ± 10	35 ± 6
18	LD-333	1	E78°59′42.4″	N30°18′02.2″	205.9	4.5	13.1	1.5	78 ± 18	60 ± 8	3.3 ± 0.2	23 ± 6	18 ± 3
19	LD-453	6	E79°2′17.7″	N30°18′25.1″	157.9	2.7	19.4	2.6	64 ± 19	50 ± 3	4.3 ± 0.2	15 ± 4	12 ± 1
Dhari													
20	LD-376	13	E78°52′31.2″	N30°15′14.3″	129.9	2.9	6.3	1.6	88 ± 21	70 ± 1	2.6 ± 0.1	34 ± 7	27 ± 2
21	LD-377	11	E78°52′31.2″	N30°15′14.3″	129.9	5.5	8	1.7	114 ± 52	68 ± 3	3.3 ± 0.2	34 ± 16	20 ± 2
Srinagar													
22	LD-327	10	E78°47′50.3″	N30°13′48.4″	137.2	4.3	12.8	2.0	69 ± 19	56 ± 7	3.6 ± 0.3	19 ± 5	15 ± 2
23	LD-328	3	E78°47′50.3″	N30°13′48.4″	176.8	3.4	12.8	2.1	60 ± 8	52 ± 3	3.6 ± 0.4	16 ± 3	14 ± 1
24	LD-338	5	E78°48′21.3″	N30°13′13.5″	159.5	3.1	7.1	1.6	39 ± 5	33 ± 1	2.7 ± 0.2	14 ± 2	12 ± 1
25	LD-380	4	E78°49′16.3″	N30°14′29.1″	168.5	5.3	15.3	2.3	154 ± 57	111 ± 1	4.3 ± 0.3	36 ± 13	26 ± 2
26	LD-381	2	E78°49′16.3″	N30°14′29.1″	188.6	5.4	8.9	1.1	53 ± 17	32 ± 1	2.9 ± 0.2	19 ± 6	11 ± 1
Deoprayag													
27	LD-18A	5	E78°49′29.4″	N30°08′1.6″	150	3	10.5	2	34 ± 3	–	3.3 ± 0.3	–	10 ± 2.0
28	LD-19A	33	E78°49′29.4″	N30°08′1.6″	150	3.7	19	2.6	49 ± 7	–	2.4 ± 0.1	–	12 ± 2.0
29	LD-20	37	E78°49′29.4″	N30°08′1.6″	150	4.2	41	2.9	119 ± 29	–	2.4 ± 0.1	–	18 ± 2.0
30	LD-19	70	E78°49′29.4″	N30°08′1.6″	150	3.7	11	2.2	86 ± 25	–	2.4 ± 0.1	–	21 ± 2.0
Vyas Ghat													
31	LD-567	22	E78°34′58.3″	N30°04′25.8″	116.2	2.7	14.6	2.2	90 ± 33	69 ± 7	3.6 ± 0.2	25 ± 9	19 ± 2
Chandidevi													
32	LD-286	–	–	–	180	4.6	12.0	1.5	–	–	3.4 ± 0.005	39 ± 7	11 ± 2
Fault gauge													
33	LD-490	–	E78°55′31.0″	N30°15′04.4″	163	1.2	1.5	0.2	74 ± 11	60 ± 6	0.7 ± 0.4	105 ± 17	85 ± 10

Hills at Chandi Devi temple, a sample from near the top of the alluvial cover of terrace T-4 yielded an age of 11 ± 2 ka (Sinha et al., 2009).

On the Ganga plain several sections along the Ganga River have been studied previously and here we use the chronology from the uppermost part of the exposed sections (Rao et al., 1997; Srivastava et al., 2003a,b; Tandon et al., 2006). These chronologies mark the termination of a major phase of sedimentation and subsequent incision of the upland surface of the Ganga Plain (Srivastava et al., 2003b). The location and schematic representation of the studied sites is provided in Fig. 6. At the mountain front, near Nagal, the Ganga river has incised ~18 m into its relict fan deposits, which yielded an age of 14 ± 3 ka (NN-1) near the base and 7 ± 2 ka (NN-6) near the top (Jaiswal, 2005 and our unpublished data). Shukla et al. (2001) described the sedimentary architecture of this section in detail. Further downstream, at Amroha, an aeolian dune located on the upland surface between the Ganga and the Ramganga River yielded an age of 12.3 ka (Tandon et al., 2006). This indicates that neither the Ganga nor the Ramganga has flooded this surface since ~12.3 ka and the rivers probably incised before this (Tandon et al., 2006). At Budaun the Ganga River incised the upland surface after 12 ka, as a sample ~8 m below the top of this surface yielded a quartz thermoluminescence age of 12 ± 1 ka (TL-8; Rao et al., 1997). Similarly, along the River Ganga, exposed sections towards the top of the same upland surface near Kanpur and Varanasi yielded ages of 13 ± 2 ka (GP-14, multiple aliquot additive dose protocol on quartz; Srivastava et al., 2003a,b) and 7 ± 1 ka (GP-8; SAR on quartz; Srivastava et al., 2009).

4.2. Lithofacies and sedimentation

The Quaternary fluvial deposits of the Alaknanda valley can be studied along the bluffs of terraces and can be divided into various lithofacies. The majority of the lithofacies are gravelly to sandy, and are described below using the nomenclature of Miall (1996):

4.2.1. Gcm (clast-supported massive gravel)

This lithofacies is 1–8 m thick, composed of well-rounded, imbricated, moderately to well sorted clasts. The clasts range in size from 5 to 25 cm and are dominantly composed of lithologies derived from the quartzites exposed in the Higher Himalayan region (commonly called Higher Himalayan Quartzites). The matrix is coarse to gritty, grey sand with abundant mica. These lenticular units fine upwards and often transform into coarse to medium grained horizontally laminated sand lithofacies. Laterally, the units are in places multistoried and often pass upward into grey to yellow micaceous fine sand or matrix-supported angular gravels. The average boulder population comprises 95% quartzite, 4% gneisses and ~ 1% fossiliferous Tethyan sedimentary rocks. This facies occurs commonly in all the studied sections (Fig. 7a).

The Gcm facies is a product of riverbed accretion in the form of amalgamating channel bars (Nichols, 1999; Srivastava et al., 2008). The roundness of the gravels indicates that they have undergone several cycles of weathering, erosion and deposition. The presence of medium to fine sand lenses represents the waning phase of the flood cycle. However, successive floods can erode the sandy facies and deposit another cycle of Gcm facies.

4.2.2. Gmg (matrix-supported gravel)

This lithofacies unit is 1–12 m thick, composed of poorly sorted gravel, with clasts a few centimeters to 1 m in size (maximum length). Clast imbrication is absent and the matrix is made up of fine micaceous sand and, sparingly, mud. This facies is divisible into two subfacies as follows: Subfacies A is exclusively composed of the rock types exposed in the valley walls and the clast are angular (Fig. 7b), whereas Subfacies B is made up of rounded to sub-rounded clasts of

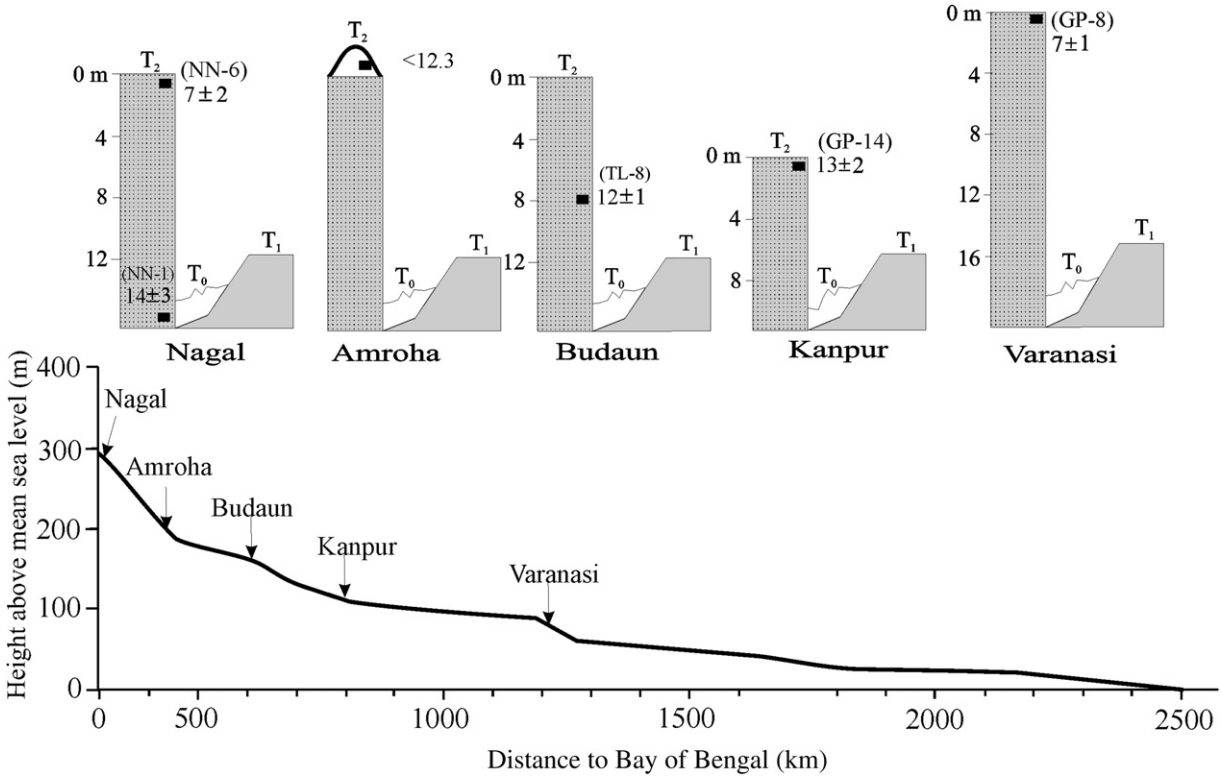

Fig. 6. Schematic sections along the Ganga River on the Ganga plain, showing the results of dating carried out to determine the age of fluvial incision. Note that the aggradation on the upland continued at least until 7 ka and the incision is younger than 7 ka. All the ages mentioned are in ka.

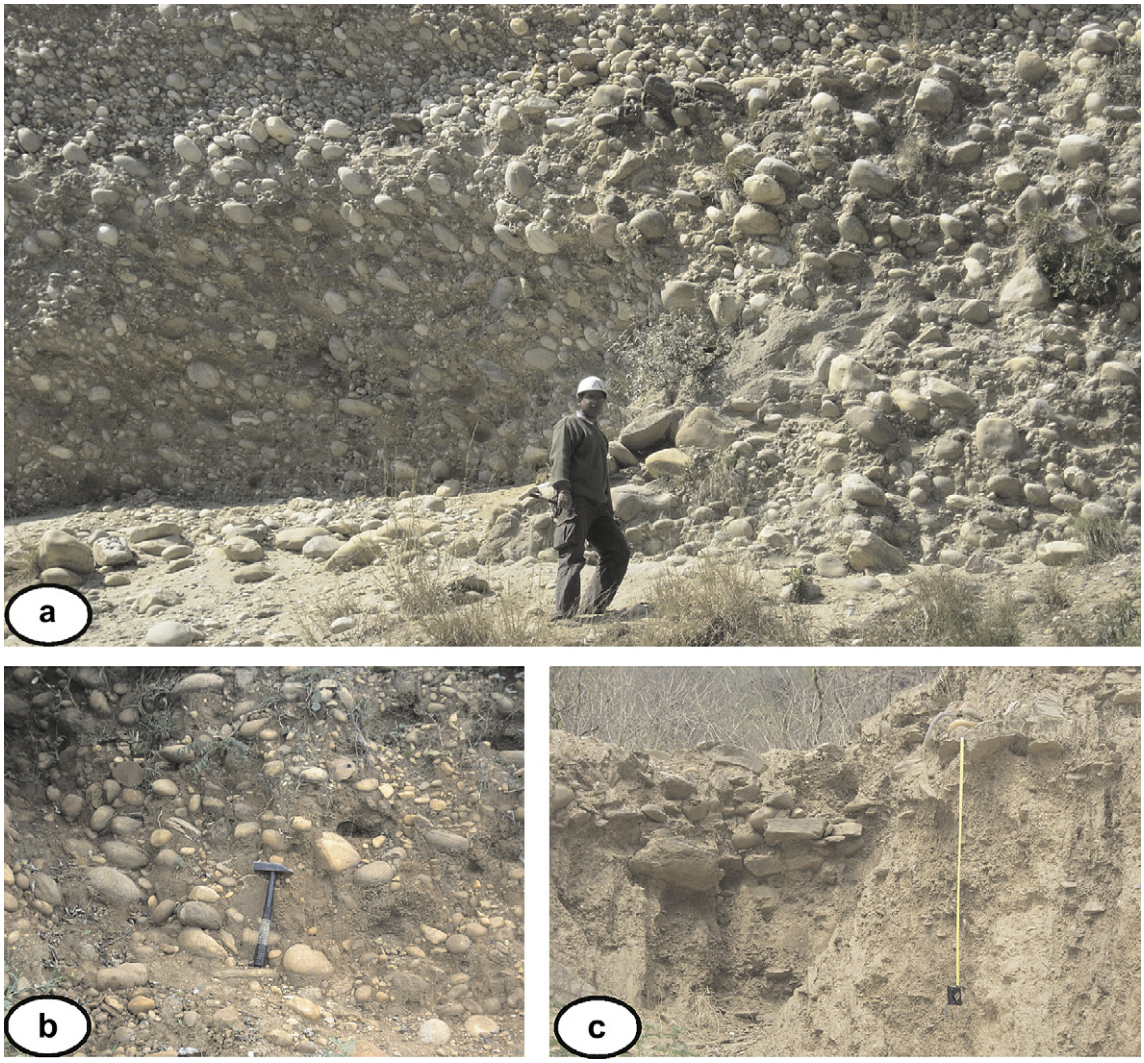

Fig. 7. Photographs showing (a) Clast-supported Massive Gravel (Gcm) lithofacies (b) Matrix-supported gravel- subfacies-A (c) Matrix-supported gravel- subfacies-B.

mixed lithologies that crop out upstream of the section (Fig. 7c). This facies is represented in every section, although any vertical facies association with a particular lithofacies has not been noticed.

These are the deposits of low-energy debris flows (Miall, 1996). Subfacies A represents the deposits of fans and landslides reaching the main channel from the immediate valley sides. In contrast, subfacies B represents debris flows that originated somewhere upstream in the catchment. The rounded to sub-rounded nature of the clasts of mixed lithologies indicates the recycling of clasts (Srivastava et al., 2008).

4.2.3. Gh (clast-supported horizontally stratified gravel)

This lithofacies is horizontally stratified and is 20–30 cm thick, having a uniform clast size of 5–6 cm. Individual beds are up to 10 cm in thickness and in general have a clast-supported and/or open framework, with little sandy matrix.

Horizontally stratified gravels form due to the migration of low-relief bedforms generated during the transition from dunes to upper stage plane beds (Miall, 1996) and represent the waning phase of floods.

4.2.4. Sh (horizontally bedded sand)

This lithofacies unit is 0.25–2.5 m thick, and is composed of horizontally laminated, medium to fine sand. These units are seen to be lenticular to sheet-like in geometry and extend for 10–100 m laterally. Individual units are in places massive and bioturbated, and may contain thin lenses comprising matrix-supported rounded boulders. The individual units may also show reddening, due to iron staining. The lithofacies is best exposed in the Deoprayag section.

These are the deposits of channel bars formed during the waning phase of floods under water depths of a few decimeters (Miall, 1996). Ferruginous reddening indicates increased aridity and subaerial exposure. The gravel lenses may indicate erosion and deposition by subsequent flood events (Srivastava et al., 2008).

4.2.5. Lithofacies associations

Lithofacies Association-A consists of lenticular to sheet-like vertically accreted gravel bodies. Individual bodies range up to ~100 m longitudinally and up to 5 m vertically. This association includes lithofacies Gcm, Gh and Sh. Lithofacies Gcm forms the basal part, followed by Gh and Sh. This association occurs laterally as lenticular units and represents channel bar migration by traction currents (Fig. 8; Srivastava et al., 2005). The vertical aggradation indicates high sediment to water ratio.

Lithofacies Association-B consists of lithofacies Gmg overlain by Sh. These are deposits of debris flows of different strengths. Their clast composition indicates the origin of the debris flows within the

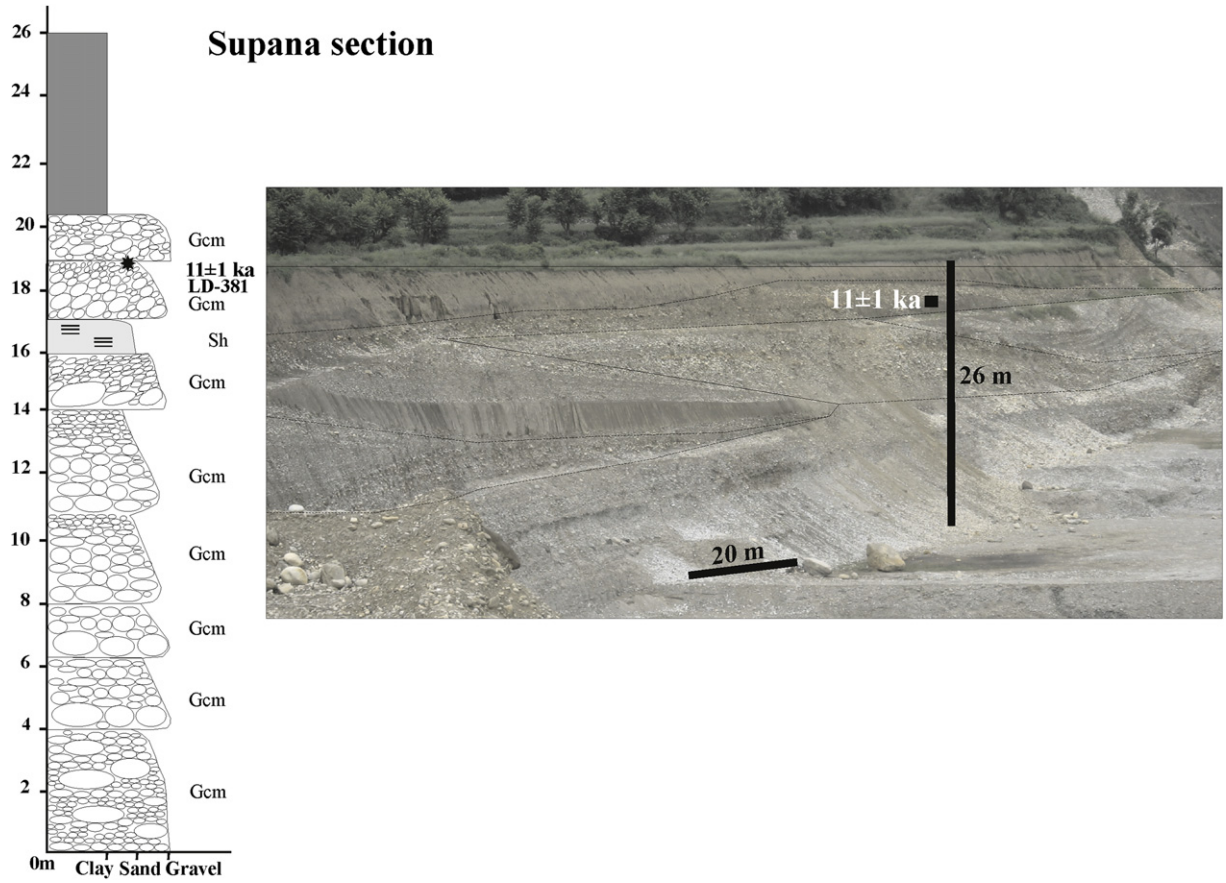

Fig. 8. (a) Litholog of the valley fill at Supana, Srinagar. (b) Photograph showing lateral geometry of the gravel units exposed at Supana near Srinagar. Note the OSL age of the sequence. Refer to Fig. 13 for location.

catchment. Flows are interpreted as locally generated, when the clast framework of Gmg facies composed mainly of locally exposed bedrock lithologies, and generated distally, in the upper part of the catchment, in such cases the constituent clasts are moderately to well rounded and are mixed with local clasts. The genetic association of Sh facies indicates temporary damming of the channel (Sundriayal et al., 2007).

The fill terraces mostly consist of channel-bound deposits grouped here as Lithofacies Association-A. The presence of rounded boulders of granite, quartzite, fossiliferous rocks and gneisses indicates that, prior to aggradation, the bedload was generated in the upper catchment located in the Higher Himalayan Crystallines and the Tethyan sedimentaries. The relative abundances of these lithoclasts depend upon the extent of exposure of the particular rock type in the catchment. The channel-bound depositional sequence may often be interrupted by the deposition of debris flows generated locally as well as distally, both of which are grouped under Lithofacies Association-B. These facies associations, in vertical sequence, are randomly associated and therefore do not carry any stratigraphic or temporal significance and suggest that the valley filling occurred via channel bar aggradation and sediments supplied from landslides and debris flows. However, at Srinagar a study indicated that the occurrence of Lithofacies Association-B is temporally associated with the phase of an enhanced monsoon (Sundriayal et al., 2007). The occasional presence of red-yellow micaceous fine sand facies, e. g. at Deoprayag, indicates development of a red profile resulting from iron oxidation due to prolonged subaerial exposure and reduced flood magnitude (Srivastava et al., 2008). The terrace sediment here is mainly derived from the Higher Himalayan Crystallines (HHC) but at times shows higher contribution of local lithologies of the Lesser Himalaya (Sundriayal et al., 2007; Srivastava et al., 2008). Sediments sourced from the HHC and deposited in the Lesser Himalayan zones represent multiple cycles of deposition and aggradation, and cannot be correlated temporally directly with phases of higher erosion in the Higher Himalayan region. In other words we can say that there was a considerable time lag between the erosion and production of sediment in the Higher Himalayan source area and the deposition of the latter as a valley fill in the Lesser Himalayan zone.

5. Morphostratigraphy of terraces

Fluvial terraces in this study have been recorded in terms of the height of the bedrock steps and the thickness of the overlying alluvial cover. Depending on the ratio of the thickness of alluvial cover and vertical bedrock incision, three different kinds of terrace configurations are identified: (I) Cut-and-fill terraces with thick alluvial cover over a shallow bedrock step; (II) terraces with almost equal thickness of alluvial cover and depth of underlying bedrock step; and (III) terraces with deeper bedrock steps and thin alluvial cover (Fig. 9).

In the following text we describe the studied sections and provide details of terrace elevation above the modern riverbed, in an upstream to downstream sequence (Figs 4 and 10). All the chronology mentioned in this section is derived using OSL on sediments of the alluvial cover.

5.1. The Nandprayag section (N30°19′59.7″ E79°18′55.0″)

This section has three levels of cut-and-fill terraces (Fig. 11). Terrace T-1 is disposed 7 m, T-2 25 m and T-3 65 m above the

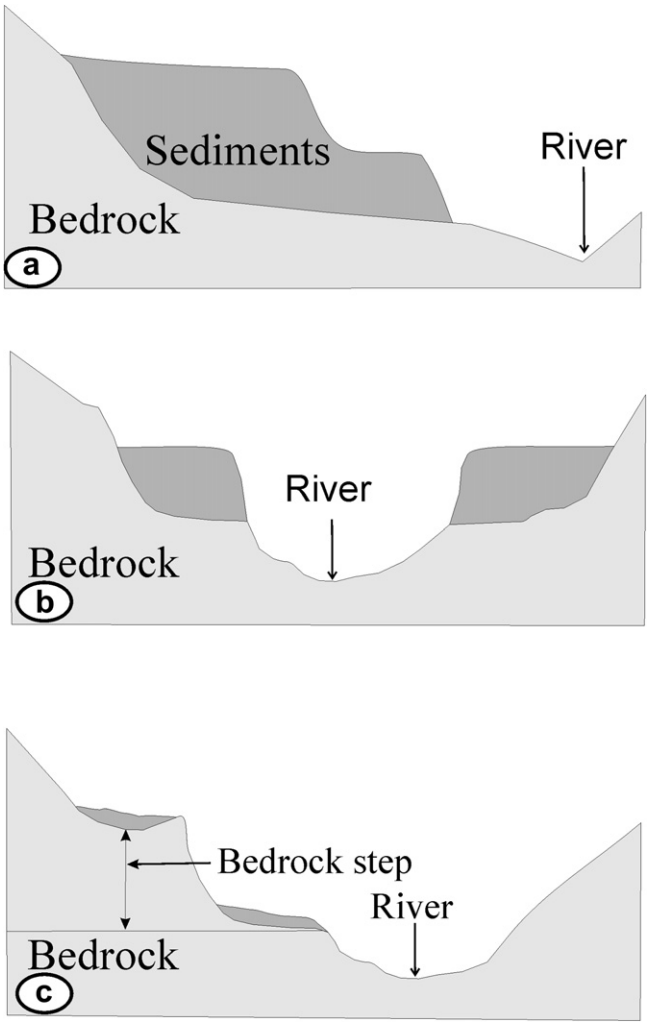

Fig. 9. Schematic section showing different types of uplift scenarios and development terraces, (I) cut-and-fill terrace (II) terraces with roughly equal depth of bedrock step and thickness of alluvial cover (III) terraces with high bedrock steps and thin alluvial cover. These indicate lower, higher and intermediate rates of uplift, respectively (see text).

modern riverbed. The bedrock step beneath T-1 reveals 2 m of fluvial incision. A sample collected from 6 m below the T-2 surface (19 m above the bedrock surface) yielded an age of 27 ± 3 ka. Thick vegetation constrained our studies of the sedimentary architecture of the fill sequence.

5.2. The Langasu section (N30°17′42.1″ E79°18′01.5″)

Three levels of cut-and-fill terraces are present on the right bank of the River Alaknanda at Langasu (Fig. 11). A 2.5 m thick bedrock step beneath T-1 reveals minor fluvial incision. The vertical separation of the deepest bedrock incision beneath T-1 and the top of the aggradational sequence is 11 m. The surfaces of T-2 and T-3 are located 36 m and 100 m above the riverbed, respectively. The riverbed here is 796 m a.s.l. A sample from 4.5 m below the top terrace T-3 yielded an age of 16 ± 2 ka.

5.3. The Seroli section (N 30°16′47.2″ E 79°14′16.8″)

This section represents a fill terrace along the river with a 16.5 m thick sedimentary fill and the base of the sequence lies 1 m above the modern riverbed (Fig. 11). The fill sequence consists of two units of Lithofacies Association-A separated by one of Lithofacies Association-B representing valley aggradation by the migration of channels bars with an intermittent locally generated debris flows (Fig. 11). A sample from 10 m below the surface of this section yielded an age of 49 ± 1 ka.

5.4. The Bamoth section (N30°16′10.7″ E79°10′17.1″)

At Bamoth, the meandering Alaknanda river is incised into the bedrock with the present-day riverbed at 732 m a.s.l. Three levels of terraces are observed on the right bank of the channel, where terraces T-3 and T-2 are of the cut-and-fill type and together form a 113 m thick valley fill sequence (Fig. 12). Total bedrock incision, punctuated with the minor aggradation of terrace T-1, is of the order of ~23 m. A sample collected from 5 m above the base of the T-2 terrace is dated to 15 ± 2 ka.

5.5. The Gaucher section (N30°17′53.4″ E79°09′34.1)

Five levels of fluvial terraces are observed on the right bank of the river at this location. Terraces T-5, T-4 and T-3 represent a first set of cut-and-fill terraces and mark an older phase of valley filling at Gaucher. The surface of terrace T-5 lies at 860 m a.s.l., T-4, which is the widest, lies at 812 m a.s.l. and T-3 lies at 770 m a.s.l. The bedrock step beneath T-3 lies at 737 m a.s.l., i.e. 24 m above the riverbed (Fig. 12). The total thickness of this phase of alluvial fill is 123 m, out of which the basal 30 m represents mainly aggradation of Lithofacies Association-A, with one event of distally generated debris flow (Fig. 12). The aggradation of the second phase comprises terraces T-1 and T-2 that are gently sloping towards the channel and are of cut-and-fill type. The bedrock surface beneath terrace T-1 lies 3 m above the riverbed at 713 m a.s.l. The total thickness of the alluvial fill represented by T-1 and T-2 is ~13 m, which is mainly in the form of Lithofacies Association-A capped by distally generated debris flow deposits representing two separate events. Samples from 24 m and 1.5 m depth below the surface of T-3 and that from near the base of T-5 indicate that the first phase of the alluvial fill occurred between 37 and 13 ± 1 ka. The age of 16 ± 2 ka at the base of T-2 is slightly overestimated as morphostratigraphically it should be younger than 13 ka. This combined evidence indicates that the Gaucher section preserves a record of nearly continuous aggradation from between ~37 and 13 ka.

5.6. The Nagrasu section (N30° 18′09.2″ E79° 07′04.7″)

Two levels of fill terraces are present on the right bank of the river at Nagrasu. The present-day riverbed is at an altitude of 686 m a.s.l. The bedrock step below the T-2 terrace lies at 99 m above the riverbed and is covered by a 20 m thick fill sequence. Similarly the base of the lower terrace T-1 lies on bedrock just 4 m above the river level, 70 m of alluvial fill taking the terrace surface to 74 m above the river level. One of the interesting facts about the deposits present here is that both are ‘rock defended’ terraces, in that both represent fossil valleys (Fig. 12). The alluvial fill of the older terrace, T-2, is mostly covered with thick vegetation and so could not be studied; however, a small sand body 6 m below the surface gave an age of 34 ± 6 ka (LD-449). The basal ~22 m of the alluvial cover of the T-1 terrace is entirely made up of Lithofacies Association-A, which, from nearly 3 m above the base, yielded an age of 13 ± 2 ka (LD-324). The data from this site indicate that aggradation phases at around ~38 ka and ~13 ka were separated by ~95 m of bedrock incision.

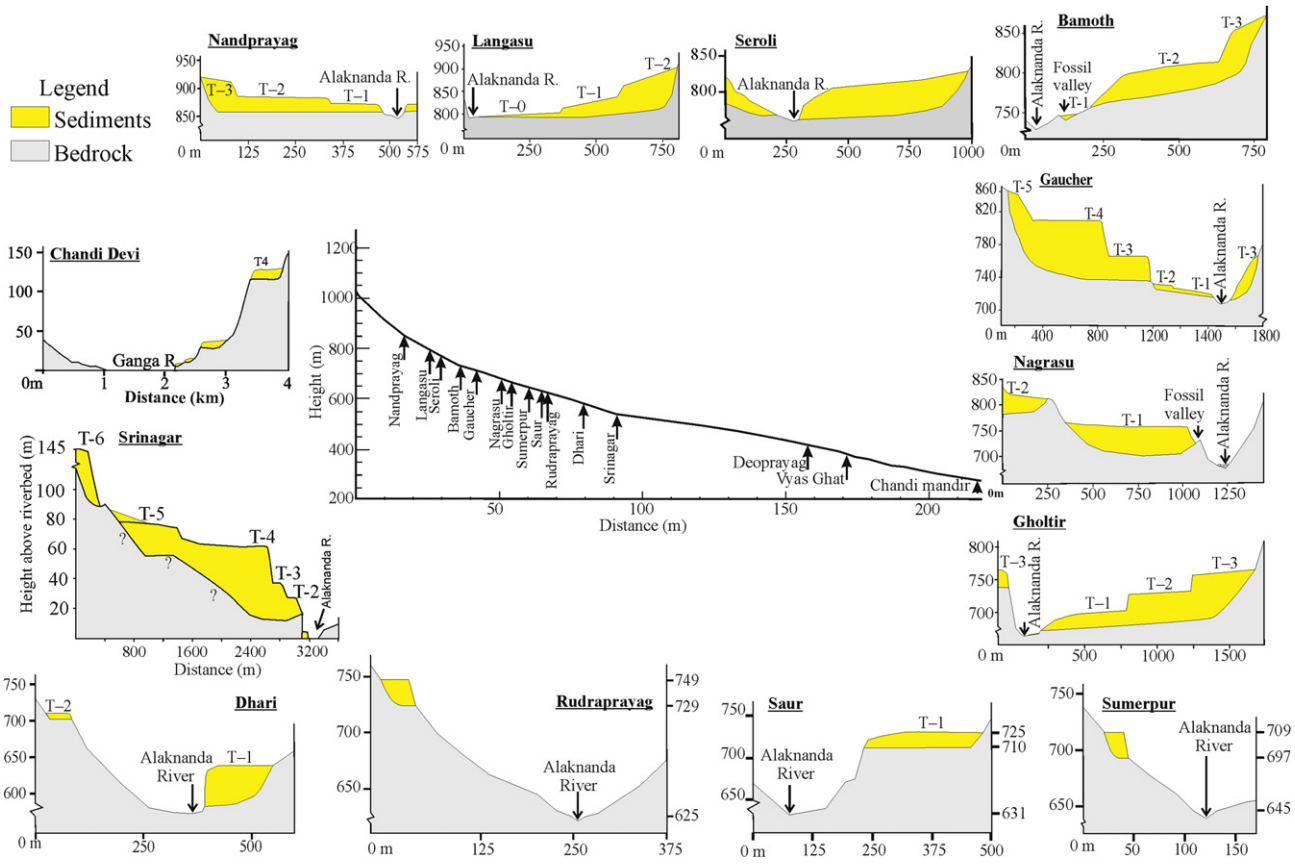

Fig. 10. Terrace configuration of the studied sections along the Alaknanda–Ganga River. Note the dominance of cut-and-fill type terraces (type I in Fig. 9) in most parts of the valley. The sections at Nagrasu, Sumerpur–Rudraprayag and Chandi Devi, however, show type III terraces (see Fig. 9) from which bedrock incision rates have been calculated (see Table 5).

5.7. The Gholtir section (N30° 18′04.4″ E79° 05′34.8″)

Three levels of cut-and-fill terraces are present at Gholtir, with the riverbed located at 673 m a.s.l. The total thickness of the alluvial fill here is 75 m, of which T-3, T-2 and T-1 account for 25 m, 40 m and 10 m, respectively; there is a 2 m thick bedrock step below T-1. Therefore this section essentially represents only a single phase of valley aggradation and minimal (2 m) bedrock incision. A ~10 m thick section of sedimentary fill, exposed at the scarp of T-1, indicates aggradation of Lithofacies Association-A. Age estimates on samples from 6.5 m below T-2 and 5 m below T-3 indicate that the aggradation took place between >40 and 11 ka and that incision of the fill post-dates 11 ka (Fig. 12).

5.8. The Sumerpur–Saur–Rudraprayag section (N30°18′25.1″ E79°02′17.7″)

At Sumerpur, where the riverbed is situated at an altitude of 631 m a.s.l., a single terrace is observed on the left bank of the river. The section here shows 84 m of limestone and dolomitic bedrock overlain by 10 m thick alluvial cover. The base (7 m below the surface) of the latter was dated to 17 ± 3 ka. Similarly, ~5 km downstream (Saur village), the same terrace, shows a bedrock step of 79 m overlain by an alluvial sequence of ~9 m. Here, a sample from 6 m below the surface was dated to 11 ± 3 ka. In the section at Rudraprayag the bedrock step, at 104 m above the riverbed, is overlain by a 12 m thick alluvial fill. The riverbed here is at 625 m a.s.l. Three samples collected from 11 m, 4 m and 1 m below the surface yielded ages of 41 ± 5 ka, 35 ± 6 ka and 18 ± 3 ka respectively. Therefore, the terrace chronology of Sumerpur–Saur–Rudraprayag section indicates aggradation between 41 and 18 ka and that this reach of the river has undergone significant local base-level adjustment by incising deep into the bedrock (Fig. 13).

5.9. The Dhari section (N30°15′14.3″ E78°52′31.2″)

A single terrace can be observed here, with a 55 m thick alluvial fill separated from the modern river by a 5 m bedrock step. The fill sequence is largely made up of Lithofacies Association-A. Two samples from 13 m and 11 m below the surface provided ages of 27 ± 2 ka (LD-376) and 20 ± 2 ka (LD-377).

5.10. The Srinagar section (N30°13′48.4″ E78°47′50.3″)

At Srinagar the Alaknanda valley is at its widest and shows the development of six terraces. Bedrock is seen below terraces T-6 and T-2, suggesting that terraces T-5–T-2 are of cut-and-fill nature. Terrace T-6 is formed by ~80 m thick alluvial fill separated from the lower terrace sequence by a 90 m thick bedrock step. The younger terrace sequence from T-5 to T-2 is composed of ~80 m thick alluvial sequence with an underlying 15 m thick bedrock step (Fig. 14). The riverbed here is 543 m a.s.l. An approximately 7 m thick fluvial fill lies over the present-day river makes terrace T-1. Thus the Srinagar section represents three phases of valley alluviation separated by two bedrock incision periods. The sedimentary architecture of older alluvial fill (T-6) is dominated by Lithofacies Association-B and a sample more than 40 m from the surface of this terrace yields an age of 26 ± 4 ka (LD-329). The younger phase of valley fill (which comprises terraces T5–T2) is dominated by Lithofacies Association-A; three samples collected from 60 m, 10 m and

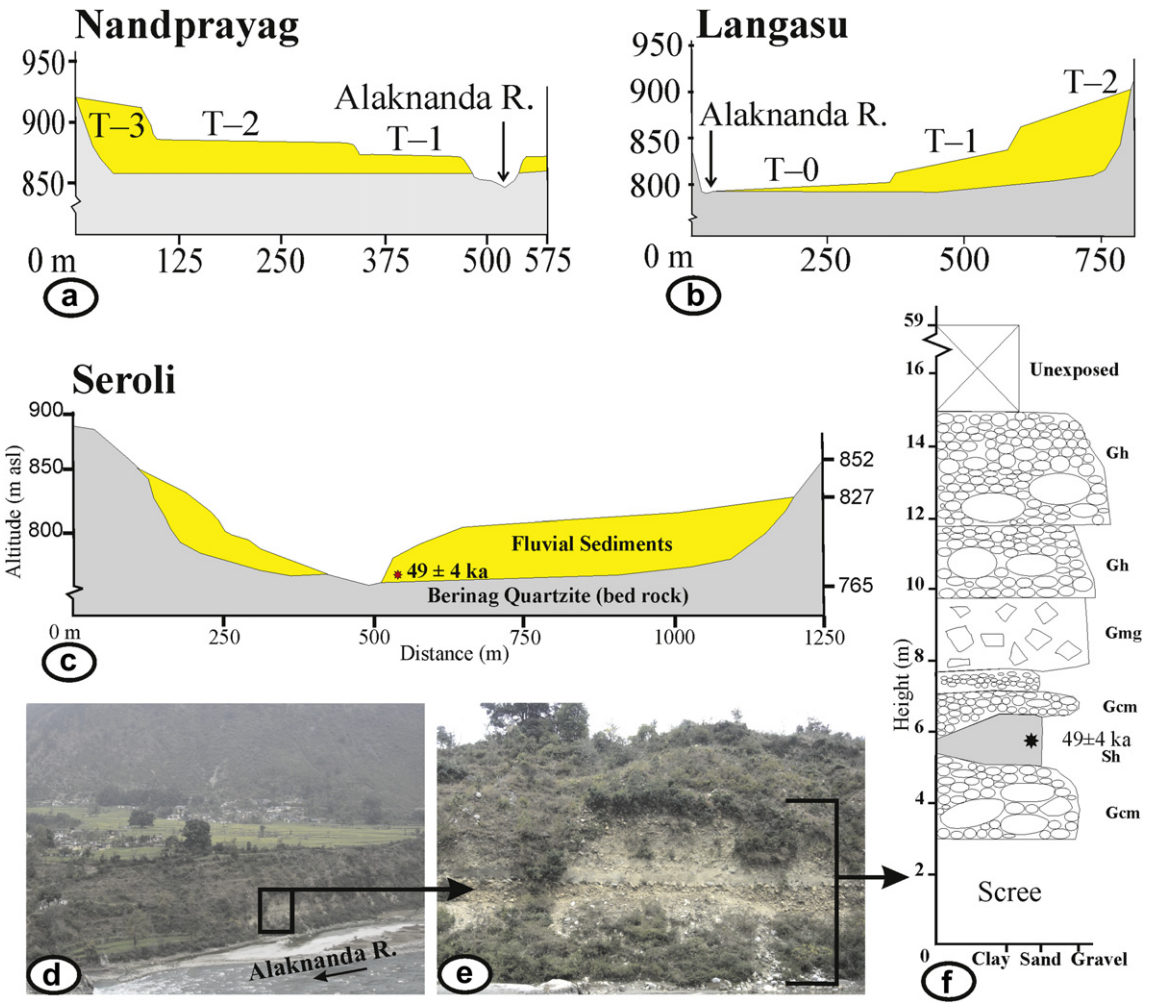

Fig. 11. The Nandprayag section (a) The Langasu section (b) The Seroli section (c) Terrace configuration. Heights are in meters a.s.l. (d) Field photograph showing alluvial fill sitting on the riverbed (e) close-up view of the alluvial fill consisting of Gcm facies (f) Litholog of alluvial cover at Seroli, showing the location of OSL samples and dating results.

3 m below the top of the fill provided ages between 17 and 14 ka. A date from near the top of a similar fill at Supana yielded an age of 11 ± 2 ka (LD-381) (Fig. 8).

5.11. The Deoprayag section (N30° 8.961′E78° 36.837′)

Srivastava et al. (2008) have studied the Deoprayag section in detail. The total thickness of the fill is ~79 m and composed of two cut-and-fill terraces. The upper T-2 lies at 86 m and the lower (T-1) at 16 m above the modern river level. A 7 m thick bedrock step lies below T-1 and above the riverbed, which here lies at an altitude of 459 m a.s.l. (Fig. 15). The fill sequence is made up of Lithofacies Association-A and includes red coloured oxidized sand. Four samples collected from 5 m, 33 m, 37 m and 70 m below the surface yielded ages of 10 ± 2 ka, 12 ± 2 ka, 18 ± 2 ka and 21 ± 2 ka respectively (Fig. 15).

5.12. The Vyas Ghat section (N30° 04′25.8″ E78°34′58.3″)

The height of the modern river at Vyas Ghat is 431 m a.s.l. The section here shows a basal ~20 m bedrock step (in Chandpur phyllite) overlain by a ~28 m thick alluvial fill. The alluvial sequence is mainly made up of Lithofacies Association-A. A sample collected from ~3 m above the bedrock is dated to 19 ± 2 ka (Fig. 16).

5.13. The Chandi Devi section

Sinha et al. (2009) have studied this section in detail. It lies in the Sub Himalaya within the Siwalik belt. The River Ganga has cut four bedrock steps here with thin alluvial cover lying over them. The uppermost terrace, T-4, is at 104 m above the present-day riverbed, with the river at 280 m a.s.l. The alluvial cover of T-4 is 24 m thick, is made up of Lithofacies Association-A and is dated to 12 ± 2 ka at 5 m below the top (Fig. 16).

6. Chronological synthesis of terraces

Thus 15 sections, from Nandprayag to Chandi Devi, covering ~200 km downstream distance, represent more than 60% of the valley length. The sections show varying degrees of aggradation and incision. The Nandprayag, Langasu and Seroli sections show minimum bedrock incision (1–2.5 m) and preserve valley fill sequences as old as 49 ka. The sections at Bamoth and Gaucher show valley fill sequences of >100 m that range in age from 37 to 13 ka. This valley reach shows >20 m of bedrock incision. Further downstream, at Nagrasu, two terraces, namely T-2 and T-1, show bedrock incision of 95 m and 4 m respectively and represent valley aggradation from 38 to 32 ka BP. The Gholtir section reveals a sedimentary fill of 40 to 11 ka with 2 m of bedrock incision. The sections at Sumerpur, Suar and Rudrapyayag show significant

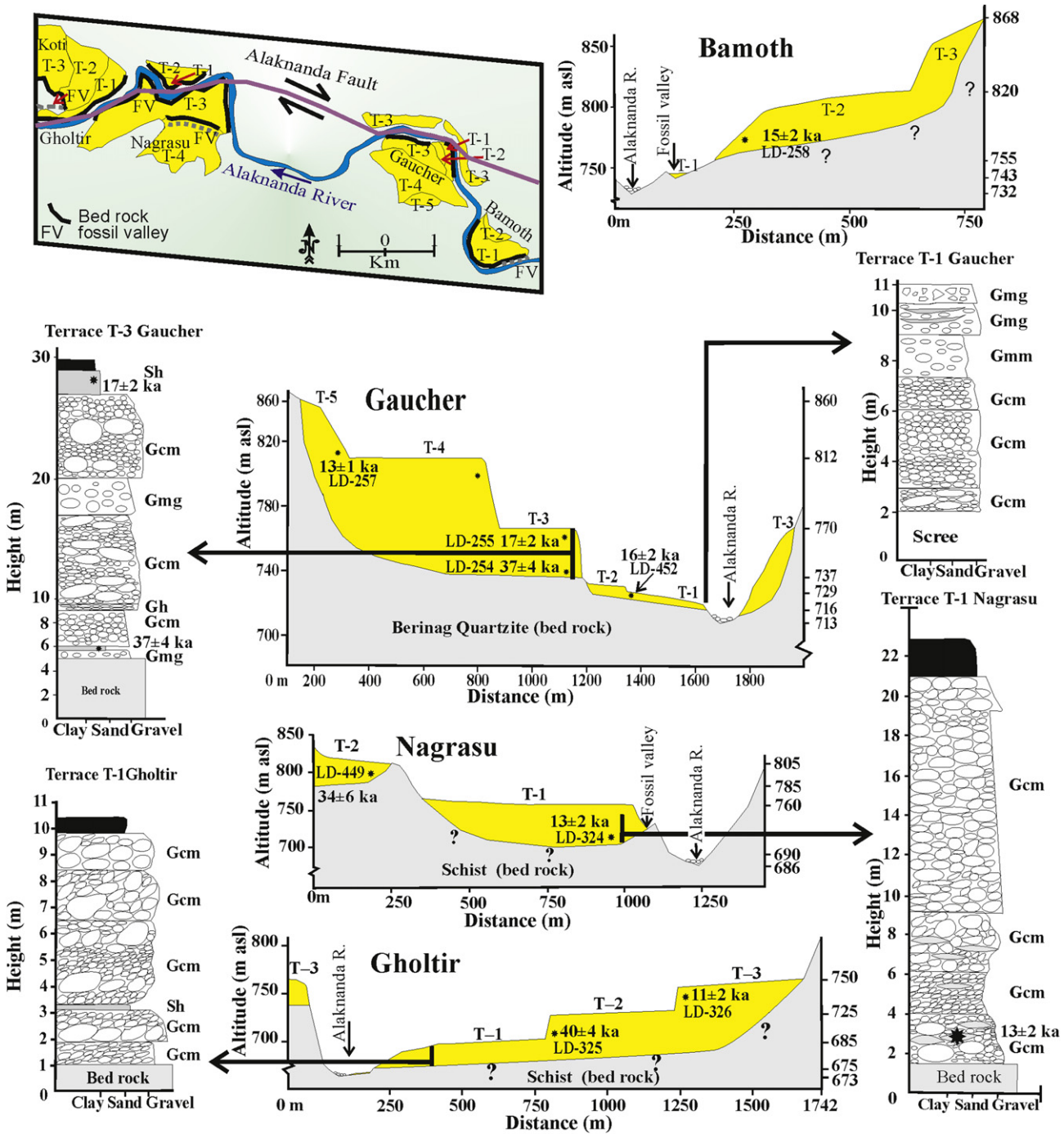

Fig. 12. (a) Field map and (b) terrace configuration (heights are in meters a.s.l.) (c) lithologs and luminescence age of alluvial cover at Bamoth, Gaucher, Nagrasu and Gholtir.

bedrock incision of 84, 79 and 104 m respectively and represent aggradation between 41 and 11 ka BP. The Dhari section shows 55 m thickness of aggradation and ~5 m of bedrock incision. Similarly the Srinagar section shows two phases of valley aggradation and bedrock incision. Here the first phase represents aggradation prior to 25 ka and the second between 17 and 14 ka. Similarly, at Deoprayag a ~79 m thick alluvial fill sits above a 7 m bedrock step, the aggradation having started before 21 ka and continued until 11 ka. The geomorphic configuration at Vyas Ghat shows a 20 m bedrock step overlain by 28 m thick alluvial fill. The latter sequence, near the base, yielded an age of ~19 ka. A section at Chandi Devi represents the geomorphic setup as the river crosses the outermost part of Himalaya. The section shows four bedrock steps, the uppermost of which lies ~104 m above the riverbed and is overlain by ~22 m of alluvial cover dated to 11 ka at 5 m below the top.

7. Discussion

7.1. Climatic variation and valley aggradation

Our observations on the geomorphic configuration of the studied reach of the Alaknanda–Ganga River combined with luminescence chronology and available data on climate change and

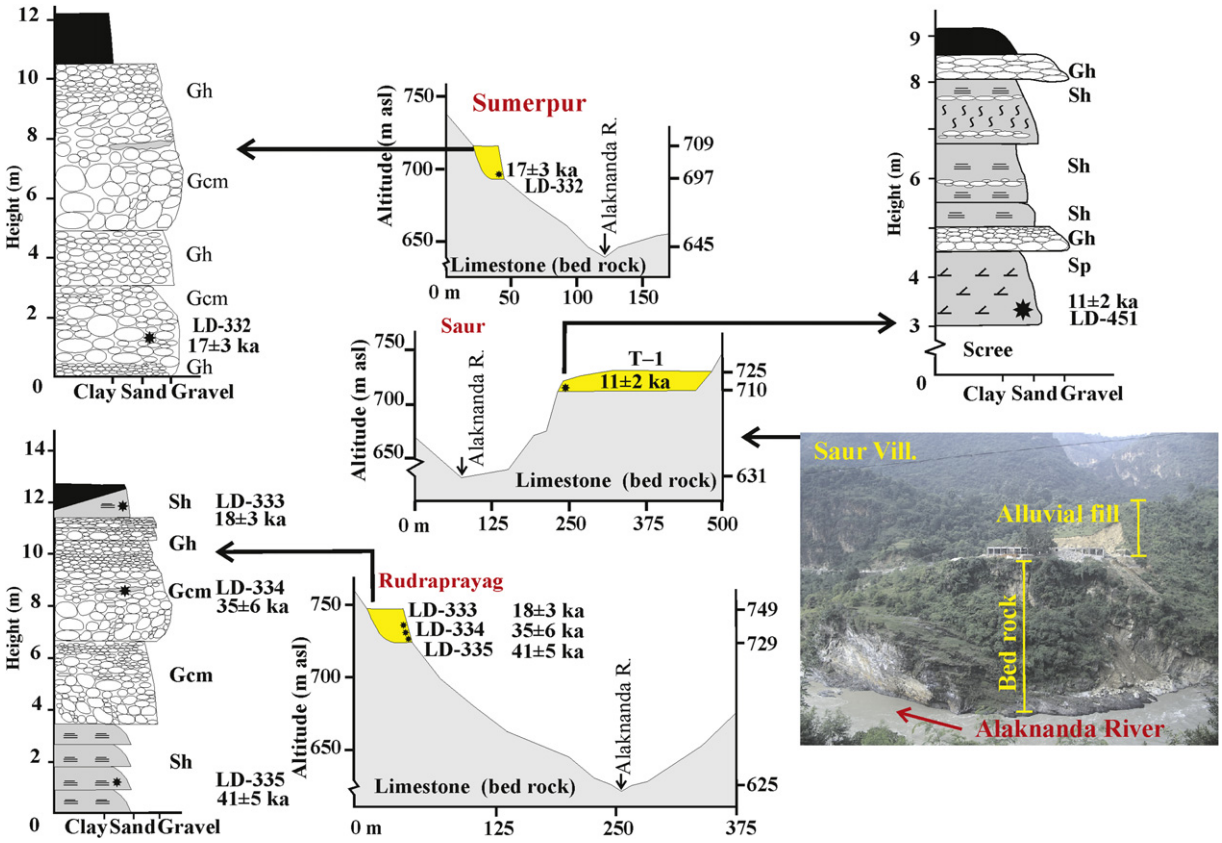

Fig. 13. Terrace configuration and litholog of alluvial cover of terraces at Sumerpur, Saur and Rudraprayag. Note the presence of deep bedrock steps and OSL ages of the alluvial cover. Heights are in meters a.s.l.

glacial advances indicate a direct link between valley alluviation and climate change. For example, glacial and deglacial processes played a significant role in supplying the sediment. The fill thickness varies from ~20 m to >125 m. These aggradational processes represent phases of high sediment generation and supply. Studies of the glacial moraines and debris fans of the upper Bhagirathi Valley indicate that deglaciation resulted in a rapid sediment transfer into the river valley (Barnard et al., 2001). The Alaknanda valley experienced two phases of major deglaciation, between 63 and 12 ka, implying that there were two periods of enhanced sediment supply. The OSL chronology of the valley fills indicate an aggradation phase that started before 49 ka and ended at ~11 ka. The ages of the alluvial fills in the Alaknanda valley group into two clusters: ~49–25 ka and ~18–11 ka (Fig. 17). The incision of the alluvial fills started soon after 11 ka. Therefore it can be inferred that the Alaknanda–Ganga River largely responded to global climatic changes and local glaciation–deglaciation conditions and the evolution of the valley fills took place as follows. (1) glaciation–deglaciation processes in the upper catchment produced large amount of sediment during ~63–12 ka; (2) Glacially produced sediment was transferred to the lower valley via several cycles of erosion and deposition during deglaciation. (3) This phase, incorporating a drier LGM and a moderately wet MIS 3, characterized by lower discharge accompanied with high sediment load, led to extensive valley aggradation in the Himalaya. (4) Climatic amelioration after the LGM at ~12 ka, and the completion of the deglaciation process, led to increased fluvial discharge and decreased sediment supply, conditions conducive to the incision of the alluvial fills.

River valley aggradation, and the subsequent formation of terraces, is assigned to varying sediment supply and/or hydrology produced by climatic perturbations (Hancock and Anderson, 2002; Srivastava et al., 2008). Sediment supply that exceeds the transport capacity of the channel will have produced the valley fills underlain by shielded bedrock erosion surfaces (bedrock steps). The number and elevation of terraces in a particular section, however, can depend upon the local tectonic setting (Wegmann and Pazzaglia, 2009). In the Alaknanda–Ganga river system, discharge conditions depend directly upon monsoonal variations and glacial melt. The sediment supply, however, is controlled by the degree of vegetation cover, glaciation–deglaciation processes and mass wasting from the steeper slopes.

Glacial expansion and retreat in the Higher Himalaya, as a major source of sediment supply, has registered two major episodes during the last 65 ka. The glacial history of the Gangotri and Satopanth, the main glaciers that feed the Ganga river system, included extensive valley glaciation during the period 63–11 ka. Deglaciation started after 11 ka, with minor re-advances at 7 ka, 5 ka, 1 ka and around 200–300 yrs BP (Sharma and Owen, 1996; Barnard et al., 2001; Owen, 2008). However, the maximum glaciation took place at ~63 ka, during which the glacier snout was located at 2600 m a.s.l. In the Alaknanda valley a three-phase glaciation is observed; the oldest Stage-1 (penultimate glaciation) descended to 2604 m a.s.l., whereas the Stage-II glaciation, corresponding with the LGM (21–12 ka), was located at 3550 m a.s.l. and the Stage-III (mid–late Holocene) remained at 3700 m a.s.l. (Nainwal et al., 2007). Glaciers in the Ganga valley registered their maximum extent at ~63 ka because this was a phase when environmental temperatures were low, but monsoons, supplying moisture, were relatively stronger than during the last glacial phase (Owen, 2008). These data, when analyzed using Arc GIS, indicate that in the Alaknanda river valley an area of approximately 2366 km^2 was vacated

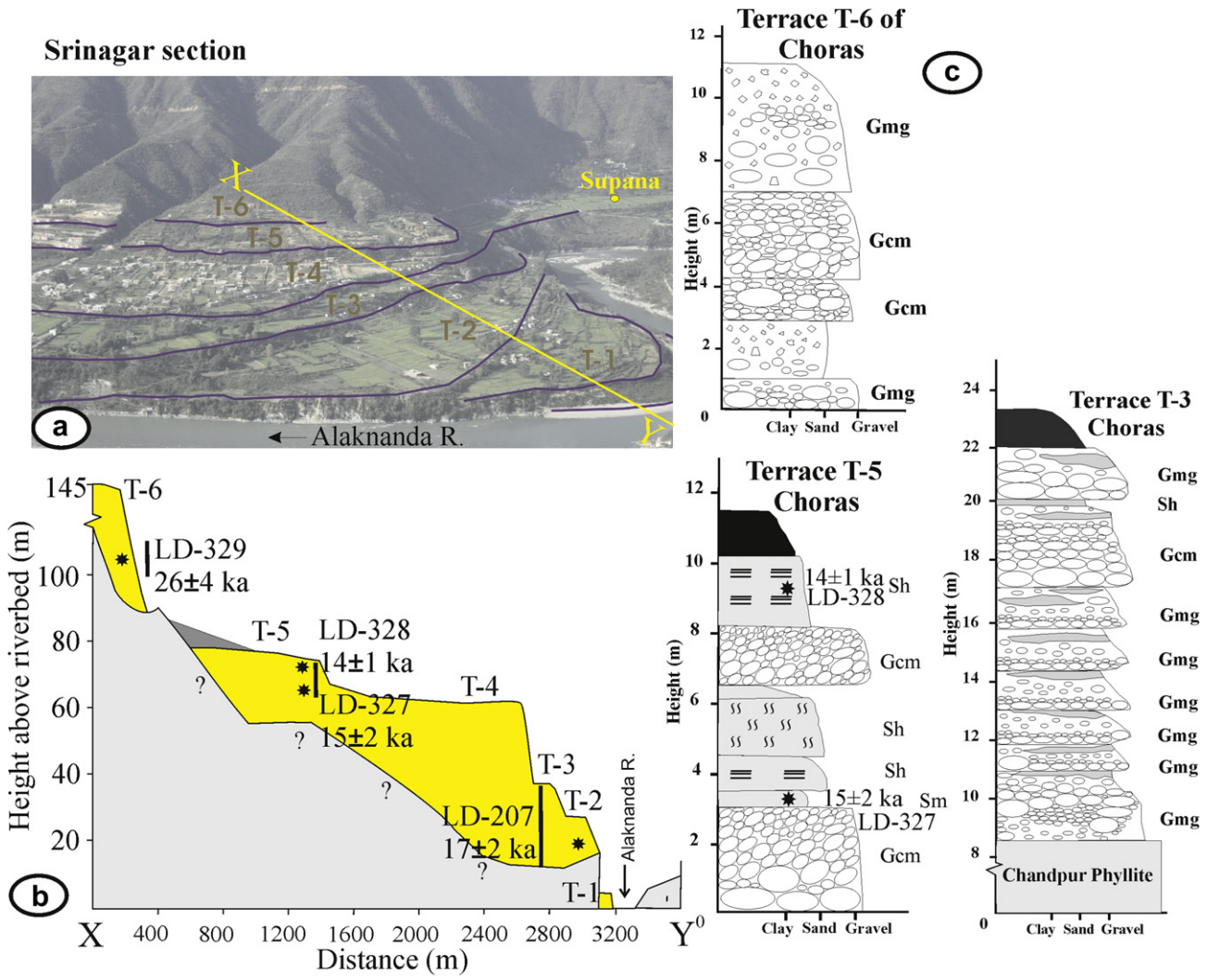

Fig. 14. (a) Photograph showing the Srinagar valley. Note the presence of six terraces. (b) Terrace configuration (vertical bar placed in the cross-section profile refers to the lithologed sedimentary profiles). (c) Lithologs of alluvial covers at Srinagar. Note location of Supana section, which is a lateral continuation of the valley fill (younger phase) preserved at Srinagar.

by glacial retreat between Stage- I and II and ~606 km^2 between Stage-II and the present day (Fig. 18). This two-phased retreat and fluvial catchment expansion would have supplied pulses of higher sediment load into the lower reaches of the river. Additionally, a study of the deposits of landslide-dammed lakes near Srinagar indicates increased landslide activity soon after the last glaciation (Sundriayal et al., 2007). Monsoon reconstructions based on a varve and rythmite sequence preserved in the upper Alaknanda catchment suggests a strengthening monsoonal system after 14.5 ka (Juyal et al., 2009).

The past variability in the Indian monsoon has been widely studied using both continental (lakes, ice cores) and marine (sediment cores) archives. A comprehensive article that analyzed the proxy records, supported with computer simulations, indicated that the precipitation over the Indian subcontinent has varied in response to Milankovitch cycles and that solar insolation, atmospheric CO_2, temperature, rainfall, vegetation cover and sediment erosion and deposition are all interlinked (Prell and Kutzbach, 1987). The study suggested that, over the Indian subcontinent, the intensity of the SW Indian monsoon and rainfall fluctuated by as much as 30% from present values over the past 100 ka (Prell and Kutzbach, 1987). During the LGM rainfall was ~30% lower than present. Computer simulations and lake and ocean records indicate that after the LGM, at ~12 ka, the monsoon started ameliorating towards a peak at around 9 ka (Cullen, 1981; Swain et al., 1983; Van Campo, 1986; Dill et al., 2003). More recent findings from the Bay of Bengal and offshore from Sumatra show that monsoonal activity after the Last Glacial Phase commenced around 15 ka BP, becoming well established 2000 years later; they also show that the Holocene saw a significant increase in river discharge to the ocean and that, in the Ganga Plain and the Himalaya, vegetation, was progressively re-established, after the Last Glacial Phase, between 19 and 8 ka (Galy et al., 2008; Murgese et al., 2008). Reconstruction of temporal variations in sea surface salinity (SSS) in the Bay of Bengal and fluvial discharge of the Himalaya during the Late Quaternary indicates that between 20 and 15 ka BP the Higher Himalaya was intensively glaciated, with minimal fluvial discharge until 15 ka BP. The beginning of the Holocene (~9.5 ka) was characterized by high fluvial discharge, attributed to an intensified monsoon regime that persisted throughout the Early Holocene (Chauhan, 2003). Overall, important climatic events during the last 60 ka coincide with MIS 3 (Marine Isotope Stage 3; 60–25 ka), which was relatively humid and cold, MIS 2 (25–15 ka), the last glacial phase (LGM); MIS 1 (12–0 ka) marks the major shift in precipitation regime from drier (glacial conditions) to wetter Holocene. Therefore, it can be concluded that from ~60 to 12 ka the hydrology of the Ganga river

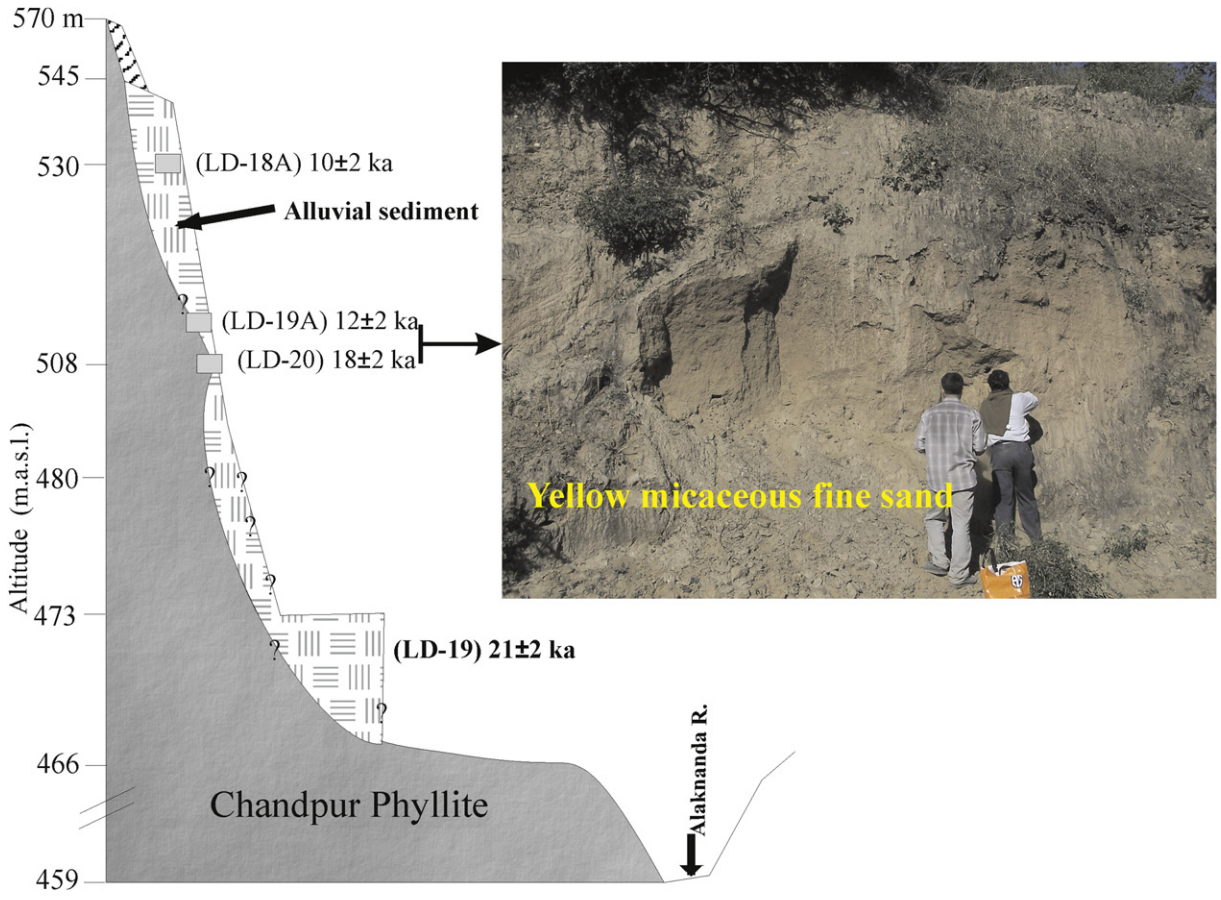

Fig. 15. Terrace configuration and litholog of alluvial cover at Deoprayag (modified after Srivastava et al., 2008). Note the presence of oxidized red coloured fine sand dated to 18 ± 2 ka. The fill dates to between 21 and 10 ka.

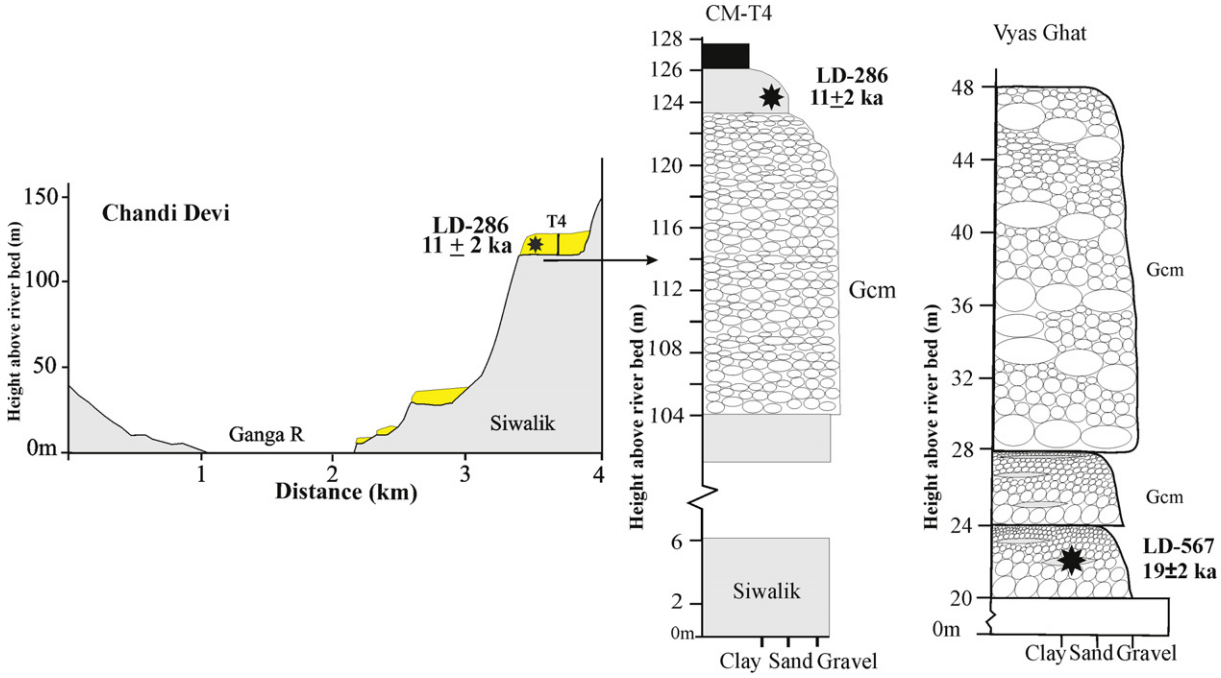

Fig. 16. Terrace configuration and litholog of alluvial cover at Vyas Ghat and Chandi Devi. Note that Chandi Devi terraces, unlike any other sections, are dominantly type III (see Fig. 9) type showing multiple phases of bedrock incision (The Chandi Devi data is from Sinha et al., in press).

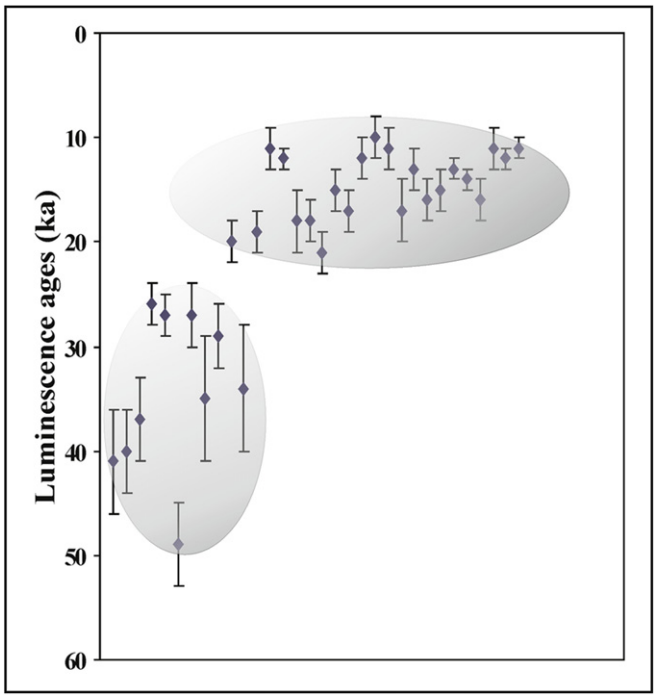

Fig. 17. Distribution of Luminescence ages of valley fill in the Ganga–Alaknanda River in the mountainous region. Note the two clusters.

system was of lower energy than at present, with a significant increase after 12 ka, peaking at ~9 ka.

A review of chronologies from all over the Himalayan catchments of the Ganga and other major river systems indicates climate change to be responsible for river incision and the formation of terraces. Well-studied rivers include the Spiti and Sutlej, in the NW Himalaya (Burbank et al., 1996; Bookhagen et al., 2005; Phartiyal et al., 2009), as well as rivers like the Kali Gandaki, the Marsyandi, the Burhi Gandaki, the Trishuli, the Sun Kosi, the Bagmati and the Arun Rivers in the Central Nepalese Himalaya, where late Pleistocene–Holocene deposits are well preserved. Fill terrace deposits in the Marsyandi river valley have been dated at around 50–35 ka, suggesting valley alluviation during same the phase as in the Alaknanda (Pratt et al., 2004). Studies on bedrock strath terraces in Central Nepal have indicated that, although the straths lie at different levels above the riverbed, their incision ages cluster between ~11 and 9 ka (Laveì, 1997; Laveì and Avouac, 2001). Likewise, in the Eastern Himalaya of Sikkim, the River Teesta incised the mountain front at 11.3 ka (Mukul et al., 2007). In the NE Himalaya, the Kameng River started to incise at 13.9 ka (Srivastava and Misra, 2008) and similar results have been obtained from the mountain exit of the Brahmaputra river (Srivastava et al., 2009). This review has indicated that in the Himalayan region river valleys experienced incision ~13–9 ka (Srivastava et al., 2009). Similar studies from other tectonically active settings, despite differing incision rates, have also demonstrated the coincidence of incision with documented climatic changes, suggesting climate change to be the major forcing factor responsible for periodic river aggradation and incision: e.g. the Charwell river in the Kaikoura Ranges, New Zealand (Bull and Knuepfer, 1987; Bull, 1991), strath and cut-and-fill terraces along the three various rivers at Mendocino triple junction, northern, California (Merritts et al., 1994; Fuller et al., 1998; Pazzaglia et al., 1998; Hancock et al., 1999) and the fluvial record preserved along the Clearwater River of the Casacadia fore arc (Pazzaglia and Brandon, 2001).

7.2. Linkages with the Ganga foreland and the Bengal Delta

The Ganga foreland basin has formed in response to the Himalayan orogeny during the middle Miocene and since then it has been filled by sediments largely eroded from the Himalaya and to some extent from the southern plateau (Singh, 1996). Sediment production, supply and deposition, however, have been a function of ongoing tectonic activity and climate changes within the orogen and the basin and therefore the sedimentary sequence of the Ganga basin and delta archives these climato-tectonic perturbations. Major rivers like the Ganga, which originate in the higher Himalaya and flow through the basin to the Bay of Bengal, act as conduits that transfer the signal from the mountains to the foreland and deltaic zones.

Several workers have studied the foreland segment of the Ganga River and established a broad geomorphic framework (Singh, 1996), chronology of various geomorphic units (Srivastava et al., 2003a; Srivastava et al., 2009), stratigraphy of interfluve and valley fill deposits (Singh et al., 1999; Gibling et al., 2005; Sinha et al., 2007), and the timing and causes of river incision (Srivastava et al., 2003b; Tandon et al., 2006). The regional geomorphic setup of the Ganga Plain indicates that most rivers, including the Ganga and associated rivers, are incised into the Upland Interfluve Surface and thus the youngest age along the cliff section of interfluve deposits exposed along the margins of the river channels marks the timing of the incision (Srivastava et al., 2003b). At Nagal, ~30 km south of the mountain front, the Ganga River has incised into a ~20 m thick sandy sequence of Upland surface. A unit 3 m below the surface yielded an OSL age ~7 ka (Jaiswal, 2005). Further downstream, near Amroha, an aeolian dune in the interfluve regions between the Rivers Ganga and Ramganga is dated to ~12 ka, implying that these rivers never inundated the interfluve surface since then and possibly incised prior to 12 ka (Tandon et al., 2006). Likewise, at Budaun the Ganga River has incised ~16 m into the Upland Interfluve Surface and a sample from ~8 m below the top of a vertical cliff yielded a thermoluminescence (TL) age of 12 ± 1 ka (Rao et al., 1997). Similarly OSL ages of 13 ± 2 ka and 7 ± 1 ka are reported from the top of the cliff sections at Bithur (Kanpur) and Varanasi (Srivastava et al., 2003a,b; Srivastava et al., 2009). These chronological data indicate that the interfluve regions were aggrading at least up to ~6–7 ka and that the Ganga River incised this surface shortly thereafter (Table 3; Fig. 6). Ages of similar order are reported from the Yamuna and associated rivers (Williams and Clarke, 1995; Singh et al., 1997). In the Ganga–Gomati interfluve, central Ganga plain, a study on abandoned channels and oxbow lakes indicated higher drainage density ~13 ka when the SW monsoon was probably stronger (Srivastava et al., 2003c) The stratigraphic succession below the Upland interfluve surface along the Ganga River at Bithur indicates a discontinuity surface related to reduced flooding at around the LGM (Gibling et al., 2005). Luminescence age data from two sedimentary cores drilled in the valley fill sequence near Kanpur reflect two distinct phases of valley aggradation before 26 ka and between 11 and 6 ka (Sinha et al., 2007). Similar investigations from other river systems of the southern Ganga Plain have indicated a decline in fluvial aggradation around the LGM (Williams et al., 2006; Gibling et al., 2008). The summed probability plots of published chronologies from the Ganga plain reveal several periods of alluviation in the Ganga foreland since the strengthening of the SW Indian Monsoon after 14 ka (Kale, 2007). To summarize, the fluvial archives from the Ganga Plain indicate the following. (1) The Ganga River incised into the uplands after 7 ka, which is 2–3 ka later than in the Himalaya. (2) There were two major sedimentary pulses from the Himalaya to the Ganga plain, which occurred before 26 ka and between 13 and 6 ka, whereas the Himalayan rivers aggraded in two phases from

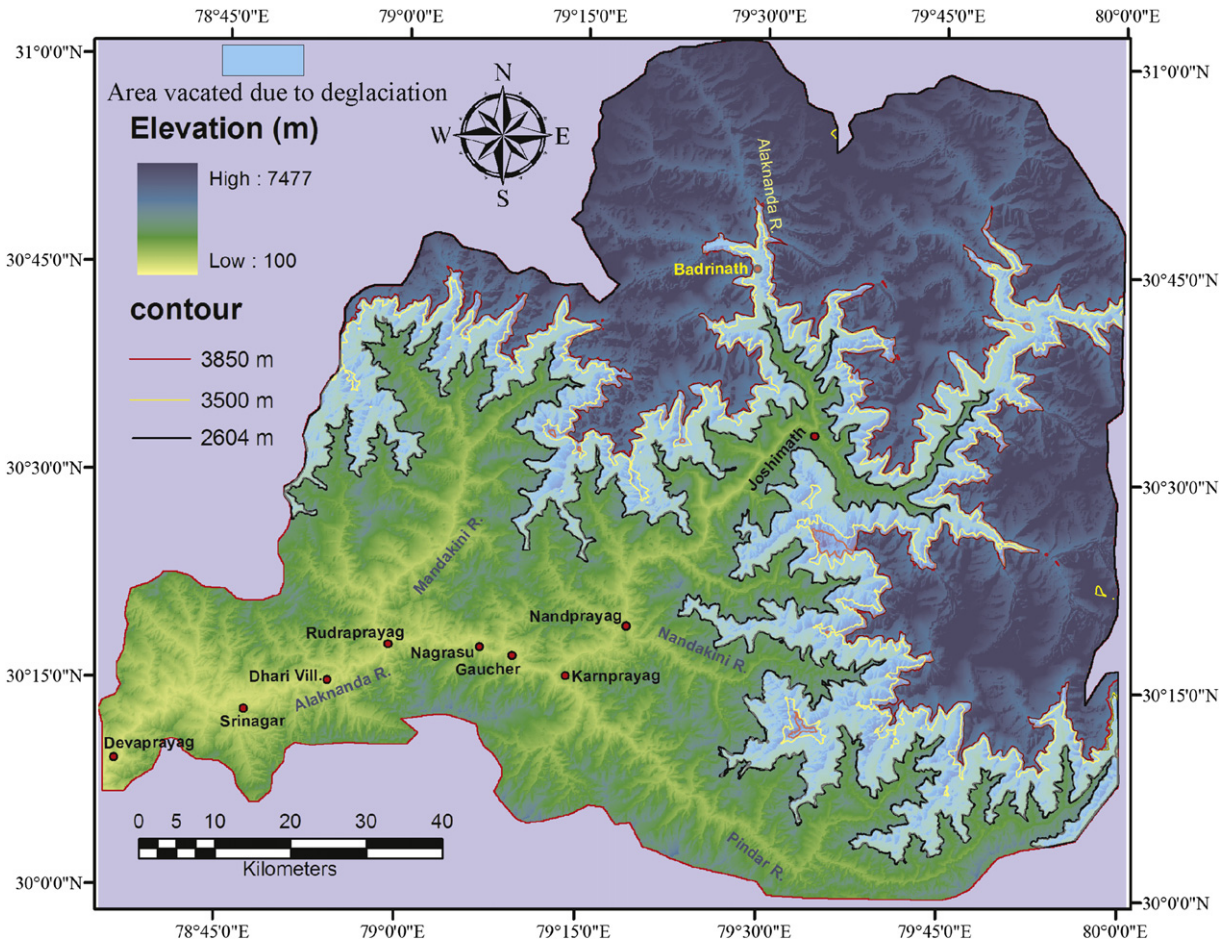

Fig. 18. Area occupied by glaciers in the Alaknanda river valley during the past ~63 ka and between ~21 and 18 ka (LGM). Note the total surface area vacated by the glaciers from ~63–0 ka.

~49 to 25 and between 18 and 11 ka. (3) The rivers experienced reduced flooding around the LGM. (4) There was increased fluvial activity in response to the climatic amelioration after the LGM.

The Bengal Delta acts as the ultimate sink into which the Ganga and Brahmaputra River systems deliver their water and sediment. The sediment budget delivered to the sink however varies with the climate and tectonism in the source region (Goodbred, 2003). Borehole studies on the lower deltaic plains indicate a phase of channel filling and high sediment supply prior to 14 ka (Umitsu, 1993). Similar evidence comes from the upper Bengal Fan (2600 m depth), where the sediment input rates drastically increased at ~15 ka and continued to increase until ~12 ka (Weber et al., 2003). Studies from mangrove sequences have indicated a two-fold increase in sediment supply from the Ganga dispersal system during 11–7 ka (Goodbred and Kuehl, 2000). More recent studies of cores from the Bengal Delta indicate the presence of a regional unconformity produced by lowered sea level (>100 m below modern sea level) during the LGM, represented by a palaeosol and valley incision. During 23–17 ka the incised valley was filled as a result of the decrease in the rate of sea level fall and higher sediment supply. At ~9 ka a rapid transgression and simultaneous monsoon intensification and related high sediment load (4–8 times than present) and water discharge inundated the lowstand surface and caused a rapid aggradation of both flood plain and estuarine valley fill deposits between 8 and 7 ka (Sarkar et al., 2009). Sea surface salinity estimates from a radiocarbon-dated sediment core from the Bay of Bengal suggest high fluvial discharges starting at 12.5 ka that continued during most of the Early Holocene (Chauhan, 2003). Summarizing the above, it can be said that (1) deltaic zones received sediments and aggraded at a higher rate during 15–7 ka, which is linked with increased rainfall after the LGM and (2) 12.5–9 ka was a time of increased fluvial discharge. Based on the data from the mountains, the Ganga foreland and the delta, a relationship in terms of aggradation and incision is established below (Table 4).

Between 63 and 11 ka glacial conditions generally prevailed, encompassing the LGM (MIS 2) and penultimate glaciation (MIS 3). The Alaknanda–Ganga River valley received huge sediment load from the two-phased deglaciation and aggraded between ~49 and 11 ka in the mountainous headwaters. The ages of sedimentation in the Alaknanda valley largely group into two clusters, 49–25 ka and 18–11 ka, indicating that sediment transport was assisted by increased discharge during the climatic transitions from dry to wet. In the Ganga foreland, the stratigraphy of the upland interfluve surface as exposed along the Ganga River suggests continuous

Table 3
River incision chronologies in the Ganga plain.

Ganga River, Ganga Plain			
Location	River	Age (ka)	Reference
Fan area, Nagal	Ganga	7 ± 2	Jaiswal (2005)
Amroha	Ganga	<12.3	Tandon et al. (2006)
Budaun	Ganga	<12 ± 1	Rao et al. (1997)
Bithur, Kanpur	Ganga	13 ± 2	Srivastava et al. (2003a,b)
Varanasi	Ganga	7 ± 1 ka	Srivastava et al. (2003a), (2009)

Table 4
Summary of the responses of Ganga–Alaknanda River from the mountains–foreland–delta during the last 63 ka. 1. Owen et al. (2008); 2. Owen (2008); 3. Sharma and Owen (1996); 4. Nainwal et al. (2007); 5. Srivastava et al. (2008); 6. Srivastava et al. (2003a); 7. Srivastava et al. (2003b); 8. Gibling et al. (2005); 9. Srivastava et al. (2009); 10. Goodbred and Kuehl (2000); 11. Sarkar et al. (2009); 12. Prell and Kutzbach (1987).

Period / Geomorphic zone	~63-11 ka	~11-7 ka	Reference
Glaciated part of Alaknanda–Ganga river valley in Himalaya	Snout elevation in Alaknanda –Ganga river valley fluctuated between 2604-3550 m amsl with the maximum glaciation being at ~63 ka. The deglaciation of ~63 ka peak lead to major northward expansion of fluvial regime.	Deglaciation completed and further northward expansion of fluvial regime.	1, 2, 3, 4 and present study
Non-glaciated lower reaches of river valleys in Himalaya	Widespread valley aggradation	Rivers incised at ~11 ka	5, Present study
Indo-Gangetic plain	Active aggradation with reduced flooding during LGM as marked by unconformities	Aggradation continued till ~7 ka with incision being younger than 7 ka	6, 7, 8, 9, Present study
Bengal Delta	Active aggradation with reduced sedimentation rates around glaciation	Rate of sediment increased to ~4-8 times	10, 11
River discharge	River discharges were low as SW monsoon was ~20% weaker as compared to modern conditions	Increasing trend peaking at ~9 ka	12
Sediment load	High sediment load was generated in the Higher Himalayan reaches due to extensive glaciation and deglaciation processes	Sediment load started decreasing due to re-establishment of vegetation cover and glacial stability. The sediment to water ratio decreased due to strengthened SW Monsoon.	10, 11
Regional climate	Two major glaciations between 63-18 ka and thereafter strengthening of SW monsoon characterize this phase. The Last Glaciation (25-18 ka) phase was arider and limited in extent than the penultimate (~63 ka). The SW monsoon strengthened after 15 ka and peaked at ~9 ka.	Largely wet conditions prevailed with minor fluctuations.	1, 2, 3, 12

aggradation from ~59 to 7 ka (Srivastava et al., 2003a,b,c; Srivastava et al., 2009) with breaks around the LGM (Gibling et al., 2005).

Between 11 and 7 ka the Indian monsoon strengthened after the LGM and the rainfall and vegetation cover increased significantly (Prell and Kutzbach, 1987). This scenario led to a decrease in sediment to water ratio and subsequent valley incision. The river in the mountains shows incision at ~11 ka, whereas incision occurred at ~7 ka in the plains. This time lag can be explained by the fact that variation in channel gradient, which controls the stream power, is significantly higher in the mountains than that in the foreland (Table 1). This was also a phase of higher sedimentation rates in the Bengal Delta.

7.3. Spatial variations in bedrock incision rates

In the Alaknanda–Ganga valley river terraces can be used to decipher bedrock incision rates. Depending on the ratio of the thickness of alluvial cover and vertical bedrock incision, different terrace configurations can be evaluated and the relative role of climate and tectonics in their formation can be deciphered (Starkel, 2003). In areas of relative tectonic quiescence, the river has higher residence time and the opportunity to aggrade, forming a thick alluvial cover over bedrock steps. The subsequent incision will give rise to cut-and-fill terraces above a low bedrock step. The terraces at Nandprayag, Langasu, Seroli, Bamoth, Gaucher, Gholtir, Dhari, Deoprayag and Vyas Ghat fall in this category and can be classified as type I. The terraces at Srinagar show two bedrock steps overlain by alluvial cover of thickness almost equalling the depth of bedrock incision in each step and thus may be classified as Type II, representing mild tectonic activity. In contrast, terraces above relatively deeper bedrock steps and with thinner alluvial cover represent fluvial reaches with intense tectonic uplift (Starkel, 2003; Srivastava and Misra, 2008). Therefore the terraces at Nagrasu, Sumerpur, Saur, Rudraprayag and Chandi Devi fall into this category and can be classified as Type III (Fig. 9).

In the present study the bedrock incision rate has been estimated from dated terraces of Type III. The heights of bedrock steps above the present-day river level or above the successive younger steps has been considered as total incision (in meters) (Pazzaglia et al., 1998; Kumar et al., 2006; Srivastava and Misra, 2008). Thus the rates of river incision are given by the ratio of the elevation difference Δh between the two successive bedrock incision phases of the river and total time elapsed (ΔT) during the incision, and can be related to tectonic uplift in the region (Pazzaglia et al., 1998). Table 5 provides the mean incision rate using the central ages and minimum incision rates using the maximum age span. The minimum incision rates, incorporating the errors associated with the ages, are 2.7 mm/year at Nagrasu to 2.6 mm/year at Sumerpur, 5.6 mm/year and 4.9 mm/year at Saur and Rudraprayag respectively. In the frontal Himalaya, the Siwalik ranges, at Chandi Devi have been incised at the rate of 7.4 mm/year.

In the area near Rudraprayag, cosmogenic radionuclide (CRN) dating of surface rock of a strath yielded bedrock incision rate of ~4 mm/year and analysis based on active landsliding, upstream of Rudraprayag, accounted for a lowering of the landscape of ~5.7 mm/year (Barnard et al., 2001). Similarly, bedrock incision rates for the Braldu River, Central Karakoram Mountains, northern Pakistan, based on CRN ages for strath terraces, range from 2 to 29 mm/year (Seong et al., 2008). Dating of abandoned river-cut surfaces in the northwestern Himalaya reveals that the Indus River has incised through bedrock at 2–12 mm/year (Burbank et al., 1996; Leland et al., 1998). In Nepal, Higher Himalayan Crystalline (HHC) rocks have been incised at ~4–8 mm/year (Lavei and Avouac, 2001). In Central Nepal, Higher Himalayan gneiss is reported to have been incised at the rate of 13 mm/year during the Holocene (Pratt et al., 2007). Maximum bedrock incision rates as reported from the Marsyandi valley, Nepal, are ~7 mm/year in the Higher Himalaya and ~1.5 mm/year in the Lesser Himalayan Mahabarat Ranges (Pratt et al., 2004). In the outer Himalayan ranges of the Siwalik, this study estimates incision rates of 7.4 mm/year, as compared to 4–6 mm/year determined from the uplifted

Table 5
Bedrock incision rates estimates at selected locations along Alaknanda River. See the Fig. 4 for locations.

S. no	Location	Height of riverbed (mamsl)	Geomorphic unit	Strath ΔH (m)	Time to incise ΔT (ka)		Incision rate mm/yr	
					Mean	Max.	Mean	Least
1	Nandprayag		Cut-fill terrace	–	–	–	–	–
2	Langasu		Cut-fill terrace	–	–	–	–	–
3	Seroli		Cut-fill terrace	–	–	–	–	–
4	Bahmoth	732	Cut-fill terrace	–	–	–	–	–
5	Gaucher	713	Cut-fill terrace	–	–	–	–	–
6	**Nagrasu**	686	One level of Strath terrace T2 and Fill Terrace T1	T2 – T1 = 95	25	35	3.8	2.7
				–	–	–	–	–
7	Gholtir	673	Cut-fill terraces	–	–	–	–	–
8	**Sumerpur**	645	Strath terrace T1	T1 – T0 = 52	17	20	3.1	2.6
9	**Saur**	631	Strath terrace T1	T1 – T0 = 79	11	14	7.2	5.6
10	**Rudraprayag**	625	Strath terrace T1	T1 – T0 = 104	18	21	5.8	4.9
11	Dhari	580	Cut-fill terraces	–	–	–	–	–
12	Srinagar		Cut-fill terraces	–	–	–	–	–
13	Deoprayag	475	Cut-fill terraces	–	–	–	–	–
14	Vyas Ghat	442	Cut-fill terraces	–	–	–	–	–
15	**Chandi Devi**	228	Four levels of Strath terraces	T4 – T0 = 104	11	14	9.5	7.4

terraces of the Ghaggar, Markanda, Shajahanpur and Kosi rivers, in the nearby area (Kumar et al., 2001). Similarly, in the Central Himalaya, Nepal, fluvial terraces on a growing anticline in the Siwaliks, along the Bagmati and Bakeya rivers, indicate uplift rates of 10–15 mm/yr (Laveì and Avouac, 2001). In the Eastern Himalaya, the Teesta river has incised the Siwalik bedrock at a rate of ~4 mm/year (Mukul et al., 2007) and in the NE Himalaya, the Kameng river has incised the Siwalik sandstone at a rate of 7.5 mm/year (Srivastava and Misra, 2008). Our bedrock incision data indicate that near Rudraprayag and Chandi Devi, which show development of terraces with high bedrock steps, implying higher incision rates, are hotspots of tectonically driven erosion. The Rudraprayag area lies in the vicinity of the seismically active Alaknanda and Kaliyasaur faults. A gouge sampled from the latter fault zone yielded an age of ~85 ka, which indicates tectonic deformation in the area. The Chandi Devi area, which lies near the mountain front, is influenced by the deformation and uplift that is taking place in response to activity along the Himalayan Frontal Thrust (HFT). Therefore, the Himalayan thrust belt has experienced tectonic deformation both near the mountain front (i.e. Chandi Devi) and in the hinterland (i.e. the Rudraprayag area). The Himalaya is considered as a critical taper wedge where the activation and successive locking of thrust faults takes place. In this context the Main Central thrust (MCT) is the oldest and inactive and the frontalmost thrust located at the toe of the wedge, i.e. Himalayan Frontal Thrust (HFT); this is an active thrust where most deformation is taking place. This is called the Forward Thrust Model, or in-sequence deformation of thrust fold belt (Dahlen, 1990). Our data however indicate that, apart from the in-sequence deformation (at Chandi Devi section), this part of the Himalaya is also registering an out-of-sequence deformation in the hinterland. Similar inferences were drawn in earlier studies where the Main Boundary Thrust (MBT, a thrust immediately older than the HFT and south of the MCT) is said to deform via normal faulting (Mugnier et al., 1994).

Bedrock incision rates are also at times equated with the landscape erosion rates. Our results indicate that basin average erosion rates differ significantly from that deduced from the terrace geomorphology (Barnard et al., 2001). Vance et al. (2003) analyzed CRN corroborated with Nd isotopic mass balance of the river sediments from the Upper Ganges catchment and indicated catchment-averaged erosion rates to be 2.7 ± 0.3 mm/yr in the High Himalaya, falling to 0.8 ± 0.3 mm/yr in the foothills. Erosion rates deduced in this study are lower than our estimates of bedrock incision rates. It should be noted in this regard that inferences drawn by Vance et al represent the erosion integrated over the whole catchment and the study also underestimated the effect of grain size variation on the ^{10}Be concentration (see Reinhardt et al., 2007). Rates estimated using bedrock steps provide site-specific information that may be governed by tectonic deformation and/or focused precipitation in the area. Furthermore, there may have been distortion of the isotopic signal as rivers like the Alaknanda, in its Lesser Himalayan stretch, have incised into their older valley fill deposits and into paleo-landslides; these older deposits, when banked against the valley walls, form barriers that restrain the entry of locally sourced sediment with Lesser Himalaya isotopic signatures. In addition, valley fills that are in general dominated by Higher Himalayan sources erode and supply sediment to the channel and add a Higher Himalayan isotopic signature in the Lesser Himalayan zones as well. Therefore, erosion rates based on isotopic studies of riverbed load and the mass balance of contributions of Higher and Lesser Himalayan rocks could be misleading (Burbank and Anderson, 2001).

8. Conclusions

The following conclusions can be drawn from this study:

1. The river geomorphology of the Alaknanda–Ganga river system shows well-developed terraces that in most cases are of cut-and-fill type. However, segments around Nagrasu, between Sumerpur and Rudraprayag and at Chandi Devi show terraces with deep bedrock steps.
2. The luminescence chronology of the alluvial fills indicates that the river has experienced massive valley filling episodes between ~49 and 25 ka and between 18 and 11 ka. These were phases when sediment supply significantly increased, probably due to the two phases of deglaciation during the last ~63 ka. Lithofacies analysis of the sedimentary fill indicates that the valley filling mainly took place due to channel bar aggradation during periods of high sediment supply and low water discharge and was thus climatically controlled.
3. Incision of the valley fill started soon after 11 ka. Increased precipitation and fluvial discharge are likely causes; this incision phase is coeval with incision chronologies reported from other parts of the Himalaya.
4. Records from the Ganga foreland and delta suggest parallels between aggradation phases in the mountains and foreland. However, the Ganga river channel in the foreland was incised

after 7 ka, thus following a time lag of ~2–3 ka compared with the Himalaya. Decreasing stream power from the mountains to the Ganga Delta is probably responsible for this time lag.

5. Bedrock incision rates, as calculated from dated alluvial covers above bedrock steps, show values that are spatially variable and fall in the range of rates reported from across the Himalaya. These estimated rates, however, are higher than the basin average erosion rates calculated using isotopic mass balance in riverbed sediments.

Acknowledgements

We thank Dr. A.K. Dubey, Director, Wadia Institute of Himalayan Geology, Dehradun for his support and encouragement. PS acknowledges Department of Science and Technology for partial financial support in the form of research grant # SR/S4/ES-139/2005. This work forms part of YR's Ph.D. thesis. Comments by Prof. David Bridgland and an anonymous reviewer helped immensely in improving the manuscript. Discussions with Dr. Navin Juyal, PRL, Ahmedabad; Prof. Y.P. Sundriyal, HNB Garhwal University, Dr. R. Islam, R. Kumar and S.K. Ghosh, Wadia Institute of Himalayan Geology helped in developing the ideas. Suggestion by Drs. Lewis Owen and Paul Hesse helped in shaping the manuscript. Sri Chandrashekhar helped with XRF analysis and Sri V.P. Gupta helped with sample preparation for OSL dating.

References

Aitken, M.J., 1998. An Introduction to Optical Dating. Academic Press, London.

Banerjee, D., Singhvi, A.K., Pande, K., Gogte, V.D., Chandra, B.P., 1999. Towards a direct dating of fault gouges using luminescence dating techniques – methodological aspects. Current Science 77, 256–269.

Barnard, P.L., Owen, L.A., Sharma, M.C., Finkel, R.C., 2001. Natural and human induced landsliding in the Garhwal Himalaya, northern India. Geomorphology 40, 21–35.

Bookhagen, B., Thiede, R.C., Strecker, M.R., 2005. Abnormal monsoon years and their control on erosion and sediment flux in the high, arid northwest Himalaya. Earth and Planetary Science Letters 231, 131–146.

Bridgland, D.R., 2000. River terrace systems in North-west Europe: an archive of environmental change, uplift and early human occupation. Quaternary Science Reviews 19, 1293–1303.

Bridgland, D.R., Westaway, R., 2007. Preservation patterns of Late Cenozoic fluvial deposits and their implications: results from IGCP 449. Quaternary International 189, 5–38.

Bull, W., 1991. Geomorphic Response to Climatic Changes. Oxford University press, 326 pp.

Bull, W.B., Knuepfer, P.L.K., 1987. Adjustments by the Charwell River, New Zealand, to uplift and climatic changes. Geomorphology, 15–32.

Burbank, D.W., Anderson, R.S., 2001. Tectonic Geomorphology. Blackwell Science, Massachusetts, 274 pp.

Burbank, D.W., Leland, J., Fielding, E., Anderson, R.S., Brozovic, N., Ried, M.R., Duncan, C., 1996. Bedrock incision, rock uplift and threshold hillslopes in the northwestern Himalayas. Nature 379, 505–510.

Chauhan, O.S., 2003. Past 20,000-year history of Himalayan aridity: evidence from oxygen isotope records in the Bay of Bengal. Current Science 84, 90–93.

Church, M., Slaymaker, O., 1989. Disequilibrium of Holocene sediment yield in glaciated British Columbia. Nature 337, 452–454.

Cullen, J.L., 1981. Microfossil evidence for changing salinity patterns in the Bay of Bengal over the last 20000 years. Palaeogeography, Palaeoclimatology, Palaeoecology 35, 315–356.

Dahlen, F.A., 1990. Critical taper model of fold and thrust belt and accretionary wedge. Annual Review of Earth and Planetary Sciences 18, 55–99.

Dill, H.G., Khadka, D.R., Khanal, R., Dohrmann, R., Melcher, F., Busch, K., 2003. Infilling of the younger Kathmandu–Banepa intermontane lake basin during the Late Quaternary (Lesser Himalaya, Nepal): a sedimentological study. Journal of Quaternary Science 18, 41–60.

Duller, G.A.T., 2008. Single-grain optical dating of Quaternary sediments: why aliquot size matters in luminescence dating. Boreas 37, 589–612.

Fuller, I.C., Macklin, M.G., Lewin, J., Passmore, D.G., Wintle, A.G., 1998. River response to high-frequency climate oscillations in southern Europe over the past 200 k.y. Geology 26, 275–278.

Galbraith, R.F., Roberts, R.G., Laslett, G.M., Yoshida, H., Olley, J.M., 1999. Optical dating of single and multiple grains of quartz from Jinmium rock shelter, Northern Australia: part I, experimental design and statistical models. Archaeometry 41, 338–364.

Galy, V., Francois, L., France-Lanord, C., Faure, P., Kudrass, H., PaLHSol, F., Singh, S.K., 2008. C4 plants decline in the Himalayan basin since the Last Glacial Maximum. Quaternary Science Reviews 27, 1396–1409.

Gibling, M.R., Tandon, S.K., Sinha, R., Jain, M., 2005. Discontinuity-bounded alluvial sequences of the southern gangetic plains, India: aggradation and degradation in response to monsoonal strength. Journal of Sedimentary Research 75, 369–385.

Gibling, M.R., Sinha, R., Roy, N.G., Tandon, S.K., Jain, M., 2008. Quaternary fluvial and eolian deposits on the Belan River, India: paleoclimatic setting of Paleolithic to Neolithic archeological sites over the past 85,000 years. Quaternary Science Reviews 27 (3–4), 392–411.

Goodbred Jr., S.L., Kuehl, S.A., 2000. Enormous Ganges–Brahmaputra sediment discharge during strengthened early Holocene monsoon. Geology 28, 1083–1086.

Goodbred Jr., S.L., 2003. Response of the Ganges dispersal system to climate change: a source-to-sink view since the last interstade. Sedimentary Geology 162, 83–104.

Hancock, G.S., Anderson, R.S., 2002. Numerical modeling of fluvial terrace formation in response to oscillating climate. Geological Society of America Bulletin 114 (9), 1131–1142.

Hancock, G.S., Anderson, R.S., Chadwick, O.A., Finkel, R.C., 1999. Dating fluvial terraces with ^{10}Be and ^{26}Al profiles: application to the Wind River, Wyoming. Geomorphology 27, 41–60.

Hodges, K.V., Wobus, C., Ruhl, K., Schildgen, T., Whipple, K., 2004. Quaternary deformation, river steepening, and heavy precipitation at the front of the Higher Himalayan ranges. Earth and Planetary Science Letters 220, 379–389.

Jain, M., Singhvi, A.K., 2001. Limits to depletion of blue-green light stimulated luminescence in feldspars: implications for quartz dating. Radiation Measurements 33, 883–892.

Jaiswal, M.K., Srivastava, P., Tripathi, J.K., Islam, R., 2008. Feasibility of the SAR technique on Quartz sand of terraces of NW Himalaya: a case study from Devprayag. Geochronometria 31, 45–52.

Jaiswal, M.K., 2005. Optically stimulated luminescence dating of fluvial sediments: application and implications to palaeoseismology and paleoclimatology. Unpublished Ph.D. thesis, M.S. University of Baroda, Vadodara, India, 139 pp.

Jha, V.K., 1992. Aerial remote sensing as an aid to engineering geologic investigation – a case study from Srinagar Hydel Project, Garhwal, U.P. Photonirvachak Journal of the Indian Society of Remote Sensing 20, 199–205.

Juyal, N., Pant, R.K., Basavaiah, N., Bhushan, R., Jain, M., Saini, N.K., Yadava, M.G., Singhvi, A.K., 2009. . Reconstruction of Last Glacial to early Holocene monsoon variability from relict lake sediments of the Higher Central Himalaya, Uttrakhand, India. Journal of Asian Earth Sciences 34, 437–449.

Kale, V.S., 2007. Fluvio–sedimentary response of the monsoon-fed Indian rivers to Late Pleistocene–Holocene changes in monsoon strength: reconstruction based on existing ^{14}C dates. Quaternary Science Reviews 26, 1610–1620.

Kumar, S., Wesnousky, S.G., Rockwell, T.K., Briggs, R.W., Thakur, V.C., Jayangondaperumal, R., 2006. Paleoseismic evidence of great surface rupture earthquakes along the Indian Himalaya. Journal of Geophysical Research 111, B03304. doi:10.1029/2004JB003309.

Kumar, S., Wesnosusky, S.G., Rockwell, T.K., Ragona, D., Thakur, V.C., Seitz, G.G., 2001. Earthquake recurrence and rupture dynamics of Himalayan Frontal Thrust, India. Science 294, 2328–2331.

Kumar, G., Agarwal, N.C., 1975. Geology of the Srinagar-Nandprayag area (Alaknanda Valley), Chamoli, Garhwal and Tehri Garhwal districts, Kumaon Himalaya, U.P. Himalayan Geology 5, 29–59.

Laveì, J., Avouac, J.P., 2000. Active folding of fluvial terraces across the Siwalik Hills, Himalayas of central Nepal. Journal of Geophysical Research, B, Solid Earth and Planets 105, 5735–5770.

Laveì, J., Avouac, J.P., 2001. Fluvial incision and tectonic uplift across the Himalayas of central Nepal. Journal of Geophysical Research 106, 26561–26591.

Laveì, J., 1997. Tectonique et erosion:L'apport de la dynamique fluviale a l'etude sismotectonique de l' Himalaya du Nepal central, these de 3eme cycle. Univ. Paris Vll, 225 pp.

Leland, J., Reid, M.R., Burbank, D.W., Finkel, R., Caffee, M., 1998. Incision and differential bedrock uplift along the Indus River near Nanga Parbat, Pakistan Himalaya, from ^{10}Be and ^{26}Al exposure age dating of bedrock straths. Earth and Planetary Science Letters 154, 93–107.

Maddy, D., 1997. Uplift-driven valley incision and river terrace formation in southern England. Journal of Quaternary Science 12, 539–545.

Merritts, D.J., Vincent, K.R., Wohl, E.E., 1994. Long river profiles, tectonism, and eustasy: guide to interpreting fluvial terraces. Journal of Geophysical Research 99, 14,031–14,050.

Miall, A.D., 1996. The Geology of Fluvial Deposits. Springer, Berlin.

Murgese, D.S., Deckker, P.D., Spooner, M.I., Young, M., 2008. A 35,000 year record of changes in the eastern Indian Ocean offshore Sumatra. Palaeogeography, Palaeoclimatology, Palaeoecology.

Mugnier, J.L., Huyghe, P., Chalaron, E., Mascle, G., 1994. Recent movements along the Main Boundary thrust of Himalayas: normal faulting in an overcritical wedge? Tectonophysics 238, 199–215.

Mukul, M., Jaiswal, M.K., Singhvi, A.K., 2007. Timing of recent out-of-sequence deformation in the frontal Himalayan wedge: insights from Darjiling sub-Himalaya, India. Geology 35, 999–1002.

Murray, A.S., Wintle, A.G., 2000. Luminescence dating of quartz using an improved single aliquot regenerative-dose protocol. Radiation Measurement 32, 57–73.

Nainwal, H.C., Chaudhary, M., Rana, N., Negi, B.D.S., Negi, R.S., Juyal, N., Singhvi, A.K., 2007. Chronology of the Late Quaternary glaciations around Badrinath (upper Alaknanda basin): preliminary observations. Current Science 93 (1), 90–96.

Nichols, G., 1999. Sedimentology and Stratigraphy. Blackwell Science, Malden, MA, 355 pp.
Olley, J.M., Caitcheon, G., Murray, A., 1998. The distribution of apparent dose as determined by optically stimulated luminescence in small aliquots of fluvial quartz: implications for dating young sediments. Quaternary Science Reviews 17, 1033–1040.
Owen, L.A., Caffee, M.W., Finkel, R.C., Seong, B.Y., 2008. Quaternary glaciations of the Himalayan–Tibetan orogen. Journal of Quaternary Science 23, 513–532.
Owen, L.A., 2008. Latest Pleistocene and Holocene glacier fluctuations in the Himalaya and Tibet. Quaternary Science Reviews. doi:10.1016/j.quascirev.2008.10.020.
Pal, S.K., 1986. Geomorphology of River Terraces along Alaknanda Valley, Garhwal Himalaya. B.R. Publishing Corporation, Delhi, 158 pp.
Pazzaglia, F.J., Brandon, M.T., 2001. A fluvial record of rock uplift and shortening across the Cascadia forearc high. American Journal of Science 301, 385–431.
Pazzaglia, F.J., Gardner, T.W., Merritts, D.J., 1998. Bedrock fluvial incision and longitudinal profile development over geologic time scales determined by fluvial terraces. In: Tinkler, K.J., Wohl, E.E. (Eds.), Rivers Over Rock: Fluvial Processes in Bedrock Channels. American Geophyisical Union, Washington DC, pp. 207–235.
Phartiyal, B., Sharma, A., Srivastava, P., Ray, Y., 2009. Chronology of relict lake deposits in the Spiti River, NW Trans Himalaya: implications to Late Pleistocene–Holocene climate-tectonic perturbations. Geomorphology 108, 264–272.
Pratt, S.B., Burbank, D.W., Heimsath, A., Ojha, T., 2004. Landscape disequilibrium on 1000–10,000 year scales Marsyandi River, Nepal, central Himalaya. Geomorphology 58, 223–241.
Pratt, S.B., Garde, M., Burban, D.W., Oskin, M., Heimsath, A., 2007. Bedload-to-suspended load ratio and rapid bedrock incision from Himalayan landslide-dam lake record. Quaternary Research 68, 111–120.
Prell, W.L., Kutzbach, J.E., 1987. Monsoon variability over the past 150,000 years. Journal of Geophysical Research 92, 8411–8425.
Prescott, J.R., Stephan, L.G., 1982. Contribution of cosmic radiation to environmental dose. PACT 6, 17–25.
Preusser, F., Chithambo, M.L., Götte, T., Martini, M., Ramseyer, K., Sendezera, E.J., Susino, G.J., Wintle, A.G., 2009. Quartz as a natural luminescence dosimeter. Earth Science Reviews 97, 184–214.
Rawat, R.S., 1979. Stratigraphy of the Garhwal Group around Rudraprayag, Chamoli district, Garhwal Himalaya, U.P. India. Himalayan Geology 9, 304–316.
Rawat, R.S., Varadarajan, S., 1979. The Alaknanda Thrust. Current Science 48, 864–865.
Rao, M.S., Bisaria, B.K., Singhvi, A.K., 1997. A feasibility study towards absolute dating of Indo-Gangetic alluvium using thermoluminescence and infrared stimulated luminescence techniques. Current Science 72, 663–669.
Rao, M.B.R., 1973. The subsurface geology of the Indogangetic plain. Journal of the Geological Society of India 14, 217–242.
Reinhardt, L.J., Hoey, T.B., Barrows, T.T., Dempster, T.J., Bishop, P., Fifield, L.K., 2007. Interpreting erosion rates from cosmogenic radionuclide concentrations measured in rapidly eroding terrain. Earth Surface Processes and Landforms 32, 390–406.
Sarkar, A., Sengupta, S., McArthur, J.M., Ravenscroft, P., Bera, M.K., Bhushan, R., Samanta, A., Agrawal, S., 2009. Evolution of Ganges–Brahmputra western delta plain: clues from sedimentology and carbon isotope. Quaternary Science Reviews. doi:10.1016/j.quascirev.2009.05.016.
Sastri, V.V., Bhandari, L.L., Raju, A.T.R., Dutta, A.K., 1971. Tectonic framework and subsurface stratigraphy of the Ganga basin. Journal of the Geological Society of India 12, 222–233.
Schildgen, T., Dethier, D.P., Bierman, P., Caffee, M., 2002. ^{26}Al and ^{10}Be dating of Late Pleistocene and Holocene Fill terraces: a record of fluvial deposition and Incision, Colorado Front Range. Earth Surface Processes and Landforms 27, 773–787.
Seong, Y.B., Owen, L.A., Bishop, M.P., Bush, A., Clendon, P., Copland, L., Finkel, R.C., Kamp, U., Shroder Jr., J.F., 2008. Rates of fluvial bedrock incision within an actively uplifting orogen: central Karakoram Mountains, northern Pakistan. Geomorphology 97, 274–286.
Sharma, M.C., Owen, L.A., 1996. Quaternary glacial history of the Garhwal Himalaya, India. Quaternary Science Reviews 28, 335–365.
Sharma, S., Joachimski, M., Sharma, M., Tobschall, H.J., Singh, I.B., Sharma, C., Chauhan, M.S., Morgenroth, G., 2004a. Lateglacial and Holocene environmental changes in Ganga Plain, Northern India. Quaternary Science Reviews 23, 145–159.
Sharma, S., Joachimski, M., Tobschall, H.J., Singh, I.B., Tewari, D.P., Tewari, R., 2004b. Oxygen isotopes of bovid teeth: archives of Palaeoclimatic variations in archaeological deposits of Ganga Plain, India. Quaternary Research 62, 19–28.
Shukla, U.K., Singh, I.B., Sharma, M., Sharma, S., 2001. A model of alluvial megafan sedimentation: Ganga megafan. Sedimentary Geology 144, 243–262.
Sinha, R., Bhattacharjee, P., Sangode, S.J., Gibling, M.R., Tandon, S.K., Jain, M., Godfrey, D., 2007. Valley and interfluve sediments in the southern Ganga plains, India: exploring facies and magnetic signatures. Sedimentary Geology 201, 386–411.
Sinha, S., Suresh, N., Kumar, R., Dutta, S., Arora, B.R., 2009. Sedimentologic and geomorphic studies on the Quaternary alluvial fan and terrace deposits along the Ganga exit. Quaternary International. doi:10.1016/j.quaint.2009.09.015.
Singh, I.B., 1996. Geological evolution of Ganga Plain: an overview. Journal of the Paleontological Society of India 41, 99–137.
Singh, I.B., Rajagopalan, G., Agarwal, K.K., Srivastava, P., Sharma, M., Sharma, S., 1997. Evidence of Middle to Late Holocene neotectonic activity in the Ganga Plain. Current Science 73, 1114–1117.
Singh, I.B., Srivastava, P., Sharma, S., Sharma, M., Singh, D.S., Rajagopalan, G., Shukla, U.K., 1999. Upland interfluve deposition: alternative model to muddy overbank deposits. Facies 40, 197–210.
Singh, M., Singh, I.B., Muller, G., 2007. Sediment characteristics and transportation dynamics of the Ganga River. Geomorphology 86, 144–175.
Srivastava, P., Singh, I.B., Sharma, M., Singhvi, A.K., 2003a. Luminescence chronometry and Late Quaternary geomorphic history of the Ganga Plain, India. Palaegeography, Palaeoclimatology, Palaeoecology 197, 15–41.
Srivastava, P., Sharma, M., Singhvi, A.K., 2003b. Luminescence chronology of incision and channel pattern changes in the River Ganga, India. Geomorphology 51, 259–268.
Srivastava, P., Sharma, S., Shukla, U.K., Singh, I.B., Singhvi, A.K., 2003c. Late Pleistocene–Holocene hydrological changes in the interfluve areas of Central Ganga Plains, India. Geomorphology 54, 279–292.
Srivastava, P., Brook, G.A., Marais, E., 2005. Depositional Environment of Clay Castles, Hoarusib River, Northern Namib deserts, Namibia. Catena 59, 187–204.
Srivastava, P., Bhakuni, S.S., Luirei, K., Misra, D.K., 2009. Morpho-sedimentary records from the Brahmaputra River exit, NE Himalaya: climate-tectonic interplay during Late Pleistocene-Holocene. Journal of Quaternary Science 24, 175–188.
Srivastava, P., Brook, G.A., Marais, E., Morthekai, P., Singhvi, A.K., 2006. Depositional environment and OSL chronology of the Homeb silt deposits, Kuiseb River, Namibia. Quaternary Research 65, 478–491.
Srivastava, P., Tripathi, J.K., Islam, R., Jaiswal, M.K., 2008. Fashion and phases of Late Pleistocene aggradation and incision in Alaknanda River, western Himalaya, India. Quaternary Research 70, 68–80.
Srivastava, P., Misra, D.K., 2008. Morpho-sedimentary records of active tectonics at the Kameng river exit, NE Himalaya. Geomorphology 96, 187–198.
Srivastava, R.N., Ahmad, A., 1979. Geology and structure of Alaknanda valley, Garhwal Himalaya. Himalayan Geology 9, 225–254.
SRTM, 2000. Shuttle Radar Topography Mission (SRTM). USGS, Reprocessing by the GLCF, 2004. 3 Arc Second SRTM Elevation. The Global Land Cover Facility, College Park, Maryland (Version 1.0).
Sundriayal, Y.P., Tripathi, J.K., Sati, S.P., Rawat, G.S., Srivastava, P., 2007. Landslide-dammed lakes in the Alaknanda basin, Lesser Himalaya: causes and implications. Current Science 93 (4), 568–574.
Starkel, L., 2003. Climatically controlled terraces in uplifting mountain areas. Quaternary Science Reviews 22, 2189–2198.
Swain, A.M., Kutzbach, J.E., Hastenrath, S., 1983. Estimation of the Holocene precipitation for Rajasthan, India, based on the pollen and lake level data. Quaternary Research 19, 1–17.
Tandon, S.K., Gibling, M.R., Sinha, R., Singh, V., Ghazanfari, P., Dasgupta, A., Jain, M., Jain, V., 2006. Alluvial valleys of the Gangetic Plains, India: causes and timing of incision. Incised valleys in time and space. SEPM Special Publication 85, 15–35.
Thakur, V.C., 2004. Active tectonics of Himalayan Frontal Thrust and seismic hazard to Ganga Plain. Current Science 86, 1554–1560.
Thiede, R., Bookhagen, B., Arrowsmith, J., Sobel, E., Strecker, M.R., 2004. Climatic control on rapid exhumation along the Southern Himalayan Front. Earth and Planetary Science Letters 222, 791–806.
Tyagi, A.K., Chaudhary, S., Rana, N., Sati, S.P., Juyal, N., 2009. Identifying areas of differential uplift using steepness index in the Alaknanda basin, Garhwal Himalaya, Uttrakhand. Current Science 97, 1473–1477.
Umitsu, M., 1993. Late Quaternary sedimentary environments and landforms in the Ganges delta. Sedimentary Geology 83, 177–186.
Van Campo, E., 1986. Monsoon fluctuations in two 20,000-Yr B.P. Oxygen-isotope/pollen records off southwest India. Quaternary Research 26, 376–388.
Vance, D., Bickle, M., Ivy-Ochs, S., Kubik, P.W., 2003. Erosion and exhumation in the Himalaya from cosmogenic isotope inventories of river sediments. Earth and Planetary Science Letters 206, 273–288.
Valdiya, K.S., 1980. Geology of Kumaun Lesser Himalaya. Wadia Institute of Himalayan Geology, Dehra Dun, 291 pp.
Wallinga, J., 2002. Optically stimulated luminescence dating of fluvial deposits: a review. Boreas 31, 303–322.
Wasson, R.J., Juyal, N., Jaiswal, M., McCulloch, M., Sarin, M.M., Jain, V., Srivastava, P., Singhvi, A.K., 2008. The Mountain-Lowland Debate: deforestation and Sediment Transport in the Upper Ganga Catchment. Environmental Management 88, 53–61.
Wegmann, K.W., Pazzaglia, F.J., 2009. Late Quaternary fluvial terraces of the Romagna and Marche Apennines, Italy: climatic, lithologic, and tectonic controls on terrace genesis in an active orogen. Quaternary Science Reviews 28, 137–165.
Weber, M.E., Wiedicke-Hombach, M., Kudrass, H.R., Erlenkeuser, H., 2003. Bengal Fan sediment transport activity and response to climate forcing inferred from sediment physical properties. Sedimentary Geology 155, 361–381.
Williams, M.A.J., Clarke, M.F., 1995. Quaternary geology and prehistoric environments in the Son and Belan valleys, North Central India. Memoir, Geological Society of India 32, 282–308.
Williams, M.A.J., Pal, J.N., Jaiswal, M., Singhvi, A.K., 2006. River response to Quaternary climatic fluctuations: evidence from the Son and Belan valleys, north-central India. Quaternary Science Reviews 25, 2619–2631.